https://doi.org/10.1093/plphys/kiac245 PLANT PHYSIOLOGY 2022: 190: 1365–1383

Plant Physiology®

Research Article

Ethylene augments root hypoxia tolerance via growth cessation and reactive oxygen species amelioration

Zeguang Liu ,[1,2] Sjon Hartman ,[1,3,4] Hans van Veen ,[1] Hongtao Zhang ,[5] Hendrika A. C. F. Leeggangers ,[1] Shanice Martopawiro,[1] Femke Bosman,[1] Florian de Deugd,[1] Peng Su ,[1] Maureen Hummel,[6] Tom Rankenberg ,[1] Kirsty L. Hassall ,[7] Julia Bailey-Serres ,[1,6] Frederica L. Theodoulou ,[5] Laurentius A. C. J. Voesenek[1] and Rashmi Sasidharan [1,*,†]

1 Plant-Environment Signaling, Institute of Environmental Biology, Utrecht University, Utrecht, 3584 CH, The Netherlands
2 Department of Botany and Plant Biology, University of Geneva, Geneva 1211, Switzerland
3 Plant Environmental Signalling and Development, Faculty of Biology, University of Freiburg, Freiburg 79104, Germany
4 CIBSS–Centre for Integrative Biological Signalling Studies, University of Freiburg, Freiburg 79104, Germany
5 Plant Sciences and the Bioeconomy, Rothamsted Research, Harpenden AL5 2JQ, UK
6 Department of Botany and Plant Sciences, Center for Plant Cell Biology, University of California, Riverside, California 92521, USA
7 Intelligent Data Ecosystems, Rothamsted Research, Harpenden AL5 2JQ, UK

*Author for correspondence: r.sasidharan@uu.nl
These authors contributed equally (Z.L., S.H., and H.v.V.).
†Senior author

Z.L., S.H., Hv.V., H.Z., and H.A.C.F.L designed and performed research and analyzed the data. S.M., F.B., F.D., P.S., M.H., T.R., and K.L.H. performed research and analyzed the data. J.B.S., F.L.T., L.A.C.J.V., and R.S. designed research. L.A.C.J.V. and R.S. coordinated the research and wrote the manuscript together with Z.L., S.H., and Hv.V. All authors saw and commented on the manuscript. R.S. agrees to serve as the author responsible for contact and ensures communication.

The author responsible for distribution of materials integral to the findings presented in this article in accordance with the policy described in the Instructions for Authors (https://academic.oup.com/plphys/pages/general-instructions) is Rashmi Sasidharan (r.sasidharan@uu.nl).

Abstract

Flooded plants experience impaired gas diffusion underwater, leading to oxygen deprivation (hypoxia). The volatile plant hormone ethylene is rapidly trapped in submerged plant cells and is instrumental for enhanced hypoxia acclimation. However, the precise mechanisms underpinning ethylene-enhanced hypoxia survival remain unclear. We studied the effect of ethylene pretreatment on hypoxia survival of Arabidopsis (*Arabidopsis thaliana*) primary root tips. Both hypoxia itself and re-oxygenation following hypoxia are highly damaging to root tip cells, and ethylene pretreatments reduced this damage. Ethylene pretreatment alone altered the abundance of transcripts and proteins involved in hypoxia responses, root growth, translation, and reactive oxygen species (ROS) homeostasis. Through imaging and manipulating ROS abundance in planta, we demonstrated that ethylene limited excessive ROS formation during hypoxia and subsequent re-oxygenation and improved oxidative stress survival in a PHYTOGLOBIN1-dependent manner. In addition, we showed that root growth cessation via ethylene and auxin occurred rapidly and that this quiescence behavior contributed to enhanced hypoxia tolerance. Collectively, our results show that the early flooding signal ethylene modulates a variety of processes that all contribute to hypoxia survival.

Received January 27, 2022. Accepted April 29, 2022. Advance access publication May 30, 2022
© The Author(s) 2022. Published by Oxford University Press on behalf of American Society of Plant Biologists.
Open Access
This is an Open Access article distributed under the terms of the Creative Commons Attribution-NonCommercial-NoDerivs licence (https://creativecommons.org/licenses/by-nc-nd/4.0/), which permits non-commercial reproduction and distribution of the work, in any medium, provided the original work is not altered or transformed in any way, and that the work is properly cited. For commercial re-use, please contact journals.permissions@oup.com

Downloaded from https://academic.oup.com/plphys/article/190/2/1365/6595039 by Erasmus University Library user on 29 September 2022

Introduction

Anthropogenic climate change has increased global flood frequency and severity, challenging sustainable crop production (Hirabayashi et al., 2013; Voesenek and Bailey-Serres, 2015). Submerged plants experience a limitation of CO_2 in photosynthesizing tissues, and oxygen (O_2) deprivation (hypoxia) in respiring tissues, because of impaired gas diffusion underwater (Voesenek and Bailey-Serres, 2015). Especially in roots, characterized by much lower O_2 levels (Vashisht et al., 2011; van Veen et al., 2016), mitochondrial respiration is arrested during hypoxia and glycolysis coupled to ethanolic fermentation becomes the main source of energy to fuel hypoxic cell survival (Loreti et al., 2016; Sasidharan et al., 2018). The severely reduced carbon fixation and high carbon demands of metabolic acclimation leads to severe energy reduction and carbon starvation. Paradoxically, de-submergence can further impair plant survival because returning to ambient light and O_2 levels (normoxia) coincides with excessive formation of damaging reactive oxygen species (ROS; Sasidharan et al., 2018; Yeung et al., 2018). Therefore, the rapid perception of submergence and timely activation of acclimation responses is essential for flooded plants to overcome hypoxia and re-oxygenation stress and increase chances of survival.

Flooding generates an array of endogenous signals that are perceived and processed by the plant to elicit adaptive responses (Sasidharan et al., 2018). However, accumulation of the gaseous plant hormone ethylene is considered the most robust signal for plant submergence detection (Voesenek and Sasidharan, 2013; Hartman et al., 2021). Indeed, ethylene biosynthesized during flooding is rapidly entrapped and perceived in submerged plant shoot and root tissues (Banga et al., 1996; Voesenek and Sasidharan, 2013; Hartman et al., 2019). This ethylene signal mediates a plethora of flood adaptive responses and facilitates acclimation to hypoxia in plants (van Veen et al., 2013; Sasidharan and Voesenek, 2015; Hartman et al., 2021). In addition, ethylene is essential for enhanced hypoxia survival and an augmented transcriptional induction of hypoxia-responsive genes in multiple angiosperms (Peng et al., 2001; van Veen et al., 2013; Yamauchi et al., 2014; Hartman et al., 2020). Collectively, these reports show that the rapid accumulation of ethylene during flooding makes it an indispensable signal to mount a successful hypoxic acclimation response in plants.

Mimicking this ethylene accumulation by pretreating plants with ethylene leads to enhanced hypoxia tolerance in marsh dock (*Rumex palustris*) and several *Solanum* species and is associated with elevated hypoxia signaling (van Veen et al., 2013; Hartman et al., 2020). A similar response in *Arabidopsis thaliana* (Arabidopsis) allowed the identification of an important underlying molecular mechanism in this species (Hartman et al., 2019). Ethylene contributes to hypoxia anticipation and acclimation by enhancing the production and stabilization of group VII Ethylene Response Factor transcription factors (ERFVIIs) prior to hypoxia (Hartman et al., 2019; Perata, 2020; Shi et al., 2020). The ERFVIIs are part of a mechanism that senses O_2 and nitric oxide (NO) levels through the PROTEOLYSIS6 (PRT6) N-degron pathway of proteolysis and are the principal activators of the core transcriptional hypoxia response (Gibbs et al., 2011; Licausi et al., 2011; Gibbs et al., 2014; Bui et al., 2015; Gasch et al., 2016). Ethylene can stabilize ERFVIIs by scavenging NO through induction of nonsymbiotic PHYTOGLOBIN1 (PGB1), already in ambient O_2 (normoxia). This enhanced ERFVII stability consequently augments the core transcriptional hypoxia response when O_2 levels diminish (Hartman et al., 2019, 2021).

Interestingly, while this mechanism describes how ethylene accelerates the transcriptional core hypoxia response (Perata, 2020), quantitative differences in hypoxic gene induction can be poor predictors of tolerance (Loreti et al., 2016). Moreover, it currently remains unclear which genes, proteins and processes functionally contribute to enhanced hypoxia acclimation and survival. Finally, which of these processes are modulated by ethylene to increase survival during hypoxia also remains elusive. To investigate the processes underpinning ethylene-enhanced hypoxia tolerance, we assessed the transcriptome of Arabidopsis root tips after ethylene pretreatment, subsequent hypoxia and re-oxygenation time points. We also quantified how the Arabidopsis proteome changes in response to an ethylene treatment. Our findings indicate that ethylene primarily promotes hypoxia tolerance through a collective response that includes enhanced hypoxia responses, improved ROS amelioration and cessation of root growth prior to hypoxia.

Results

Ethylene enhances cell viability during both hypoxia and re-oxygenation

An ethylene pretreatment enhances survival of subsequent hypoxia in Arabidopsis seedling root tips (Hartman et al., 2019). To uncover processes that contribute to this ethylene-enhanced hypoxic cell survival, we first investigated when root cells lose viability during hypoxia and re-oxygenation. The capacity of root tips to re-grow during hypoxia recovery (3 days) was used as a proxy for root meristem survival (Hartman et al., 2019). The results revealed that root tips of 4- and 5-day-old Arabidopsis Col-0 seedlings lose viability between 3.5 and 4.5 h of severe hypoxia, but that root tip survival is significantly prolonged after an ethylene pretreatment (Figure 1A; Supplemental Figure S1A). Importantly, Evans Blue (EB) staining for cell membrane integrity revealed that a proportion of seedlings treated with 4 h of hypoxia does not lose root tip cell viability during the hypoxia period itself, but during the first hours of re-oxygenation (Figure 1, B and C). Ethylene strongly reduced and delayed cell death during re-oxygenation (Figure 1, B and C). When the hypoxia duration was prolonged (4.5 h), cell death also occurred during hypoxia in addition to the re-oxygenation phase (Supplemental Figure S1, B and C). Together, these results indicate that during shorter hypoxia stress (4 h in our experiments) root tips mainly die during the re-oxygenation phase, whereas

Downloaded from https://academic.oup.com/plphys/article/190/2/1365/6595039 by Erasmus University Library user on 29 September 2022

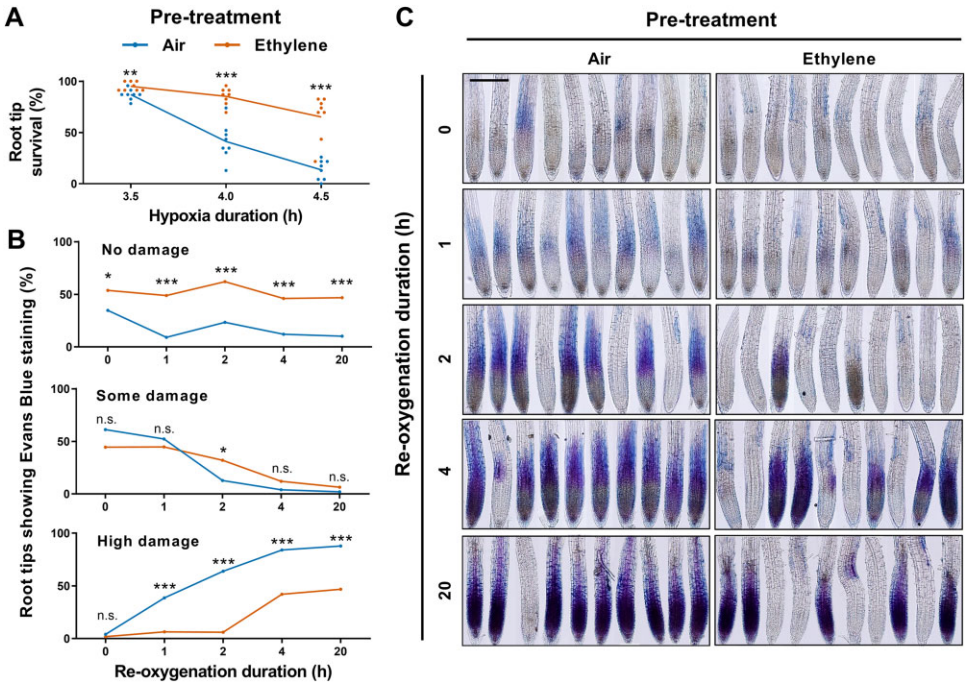

Figure 1 Ethylene pretreatment improves cell viability during hypoxia and re-oxygenation. A, Root tip survival of 4-day-old Arabidopsis (Col-0) seedlings after 4 h of air or ~5 μL·L^{-1} ethylene treatment followed by hypoxia and 3 days of recovery (n = 8 rows of 23 seedlings, Student's t test). Dots represent individual rows of seedlings. B, Classification and (C) visualization of EB staining for impaired cell membrane integrity in 4-day-old seedling root tips after 4 h of pretreatment with air or ~5 μL·L^{-1} ethylene followed by 4-h hypoxia and re-oxygenation time points. n = 44–54 root tips in (B), n = 10 random samples in (C). Classification in (B), no damage = no EB staining, some damage = detectable EB staining, high damage = clear root-wide EB staining in elongation zone and root apical meristem, (C) scale bar = 100 μm. Image in (C) is a composite of individual root pictures representing the trends in (B). For (A) and (B) asterisks indicate significant differences between air and ethylene per time point (n.s., not significant, *$P < 0.05$, **$P < 0.01$, ***$P < 0.001$, generalized linear model with a binomial error structure).

longer hypoxia (4.5 h) results in meristem death in root tips during both the hypoxia and the subsequent re-oxygenation phase. Furthermore, ethylene enhances cell survival in root tips during both the hypoxia and re-oxygenation phase.

Ethylene induces transcript abundance changes that are maintained during subsequent hypoxia

To identify the processes and associated molecular identities associated with increased hypoxia tolerance after ethylene pretreatment, microarray-based transcriptome profiling was performed (Supplemental Data, Sheets 1–7). The target tissues were root tips (0.5 cm) of 4-day-old Arabidopsis Col-0 seedlings pretreated either with 4 h of air or ethylene, and subsequently exposed to 2 and 4 h of hypoxia and 1 h of re-oxygenation (Figure 2A; Supplemental Figures S2 and S3). Interestingly, whilst the number of differentially expressed genes (DEGs) compared to the normoxic control continued to increase as the experiment progressed, the number of DEGs differing between air and ethylene (indicating an ethylene-specific effect) pretreatment decreased over time (Figure 2, B and C).

Genes that behaved differently depending on the ethylene pretreatment were of primary interest to explain differences in ethylene-mediated hypoxia and re-oxygenation tolerance (Supplemental Figure S4). Ethylene-mediated differences in expression were maximal directly after the pretreatment (Figure 2C). Of the genes that differed during hypoxia treatment, almost all were also already differentially expressed directly after the ethylene pretreatment (Figure 2, C–E). To investigate how these early ethylene effects on the transcriptome developed throughout the treatment, we grouped the ethylene pretreatment-dependent genes (differentially regulated genes [DRGs]) into 12 unique expression profiles by hierarchical clustering (Figure 2, D and E).

Seven distinct profiles were associated with a strong downregulation of transcripts by ethylene that either strengthened or counteracted responses to hypoxia and re-oxygenation (D1-7; Figure 2D). A reverse pattern, where clusters were enhanced by ethylene, was found in five profiles (U1-5, Figure 2E). In none of these clusters were the pretreatment differences further increased or decreased during hypoxia. Though these DEGs were mostly maintained during hypoxia, the difference between air and ethylene pretreatment typically declined over time (Figure 2, D and E). We conclude that the induction of ethylene signaling prior to hypoxia induces a major transcriptome reconfiguration in root tips and that most of these changes are maintained during subsequent hypoxia, and to a lesser extent during re-oxygenation.

We also identified hypoxia- and re-oxygenation-responsive processes that were not modulated by the ethylene pretreatment (Supplemental Figure S5). The hypoxic induction

Downloaded from https://academic.oup.com/plphys/article/190/2/1365/6595039 by Erasmus University Library user on 29 September 2022

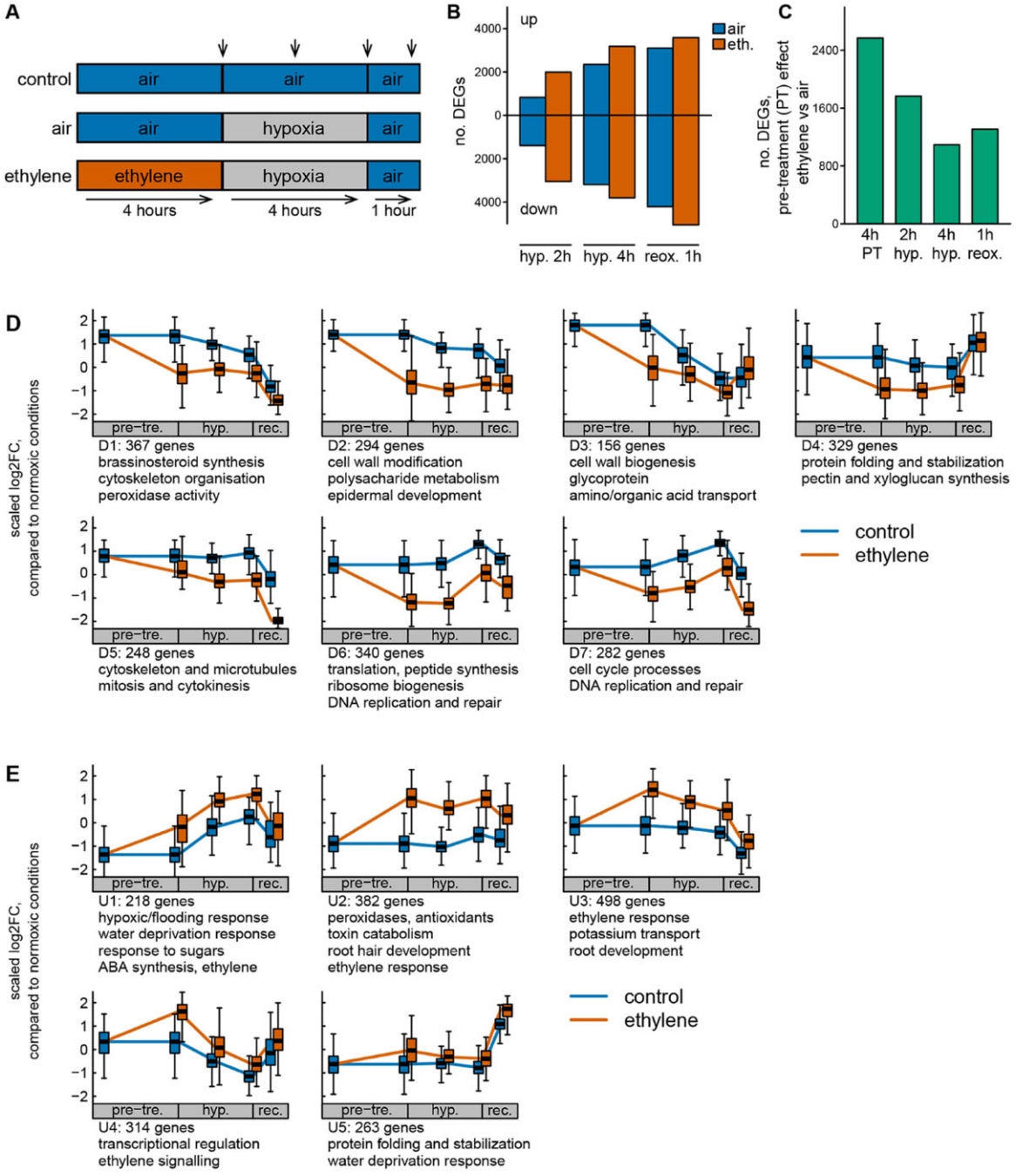

Figure 2 Ethylene leads to transcript changes that are maintained during hypoxia and re-oxygenation. A, Schematic overview of the experimental design, where arrows indicate the sampling timepoints. Arabidopsis (Col-0) 4-day-old seedlings were pretreated with air or ethylene (5 $\mu L \cdot L^{-1}$) and subsequently exposed to 4-h hypoxia (O_2 levels reach 0% after ~40 min after the start of treatment) and 1 h of normoxia in the dark. Approximately 184 root tips (< 0.5 mm from tip) were harvested per experimental replicate ($n = 3$) after the pretreatment, 2 and 4 h of hypoxia and 1 h of re-oxygenation. Significance was determined by limma linear model and Benjamini–Hochberg correction. B, The number of DEGs ($P < 0.001$) relative to the controls (air-normoxia) of the same timepoint for both air and ethylene pretreatment. C, The number of DEGs ($P < 0.001$) between air and ethylene pretreated plants, for each harvest time point. D and E, Clusters from hierarchical clustering. Boxplot details: center line, median; box limits, upper and lower quartiles; whiskers, 1.5 × interquartile range, data points outside whiskers not drawn. Key processes and functions enriched in each cluster based on GO enrichment. Full lists of DEGs per cluster and associated GO terms are available in the Supplemental Data, Sheets 1–4. Shown FCs are relative to the normoxic control of the corresponding timepoints, and were mean and standard deviation scaled by gene.

Downloaded from https://academic.oup.com/plphys/article/190/2/1365/6595039 by Erasmus University Library user on 29 September 2022

of transcripts that continued during the re-oxygenation were associated with protein folding and hypoxia, heat, and ROS responses. Genes that were continuously downregulated during hypoxia and re-oxygenation were associated with ion transport and root development. These genes may be important for acclimation to hypoxia and re-oxygenation but are unlikely to be involved in ethylene-mediated hypoxia tolerance. To better understand the influence of ethylene on transcript abundance, we went on to consider individual DRGs.

Ethylene elicits a transcript level changes that are associated with root growth cessation, ROS homeostasis, and stress responses

The nature of the genes present in each cluster (Figure 2, D and E) was assessed by gene ontology (GO) enrichment analysis. Widespread ethylene signaling-related GO terms were detected in the ethylene-enriched clusters (U1–U4; Figure 2E). Additional ethylene-enhanced GO terms included hypoxic/flooding responses, response to sugars, ABA biosynthesis (U1), toxin catabolism, antioxidants (U2), and root development (U3). Ethylene-downregulated GO terms were indicative of a general reduction in root growth, development, and cellular maintenance, including brassinosteroid biosynthesis (D1), cell wall biogenesis (D3), mitosis and cytokinesis (D5), translation and ribosome biogenesis (D6), and cell cycle (D7).

Ethylene is an established inhibitor of root growth and development (Le et al., 2001), and both known and previously unknown ethylene-driven gene clusters and genes indicative of ethylene-mediated growth cessation were identified. Ethylene suppresses root cell enlargement in the elongation zone and the epidermis through auxin signaling (Růžička et al., 2007; Swarup et al., 2007; Vaseva et al., 2018). Accordingly, cluster U3 contained known ethylene-mediated players in auxin upregulation and transport, including *ANTHRANILATE SYNTHASE α1* (*ASA1*), *ERF1*, and *HOMEOBOX52* (Mao et al., 2016; Miao et al., 2018). Cluster D2 was enriched in genes associated with cell wall modification being suppressed by ethylene. Apart from limiting growth by elongation, ethylene is also reported to reduce cell proliferation (Street et al., 2015). Accordingly, ethylene pretreatment led to downregulation of mitosis, DNA replication and cyclin genes in clusters D5, D6, and D7.

In addition to known ethylene-mediated growth suppressing pathways, our results revealed effects on growth regulators not previously associated with ethylene signaling. The development of the root relies heavily on the PLETHORA (PLT) 1 and 2 transcription factors (Aida et al., 2004; Galinha et al., 2007), the GRAS family proteins SCARECROW (SCR) and SHORTROOT (SHR; Sozzani et al., 2010), TEOSINTE-BRANCHED CYCLOIDEA (TCP) 20/21 (Shimotohno et al., 2018) and SHORT HYPCOTYL (SHY) 2 (Tian and Reed, 1999). Notably, these growth stimulating genes, *PLT1* (D7), *PLT2* (D5), *SCR* (D1), *SHR* (D3), *TCP21* (D2), and *SHY2* (D6) were all downregulated after ethylene treatment. Genes associated with biosynthesis of the root growth stimulating hormone brassinosteroid (D1) were also downregulated by ethylene (Müssig et al., 2003). Moreover, genes associated with biosynthesis of the root growth suppressor ABA were induced (U1) alongside many SNF-RELATED PROTEIN KINASE 2s (SnRK2s) (2.6 U1; 2.7 U3; 2.9 U4; 2.10 U1) that mediate ABA and stress-induced root system architectural changes (McLoughlin et al., 2012; Kawa et al., 2020). Together these results indicate that ethylene leads to mRNA transcript changes that are indicative of growth cessation in the root tip, which are maintained during hypoxia and re-oxygenation.

Ethylene also caused differential regulation of genes associated with ROS homeostasis and antioxidant activity that modulate root growth and oxidative stress responses. (Figure 2, C and D; D1, U2) (Supplemental Figure S6). These included *UPBEAT1*, a transcription factor that stimulates cell proliferation and root growth by diminishing superoxide levels through the suppression of peroxidases (Tsukagoshi et al., 2010) and previously linked to waterlogging tolerance in rapeseed (*Brassica napus*) through growth repression (Guo et al., 2020). *UPBEAT1* was ethylene induced (U4), whilst its direct target peroxidase was ethylene suppressed (D1). Ethylene downregulated *MYB30* (D1), a ROS-inducible root growth stimulating transcription factor that stimulates cell proliferation (Mabuchi et al., 2018). Collectively, this behavior of key transcription factors and genes, controlling or mediated by ROS, suggest that root growth could be reduced by ethylene through modulating ROS production (D1) and scavenging (U2).

Ethylene also controls many stress-related genes, culminating in cluster U1, where an initial transcript induction by ethylene was further continued during hypoxia. These included a range of genes classically associated with hypoxia, such as *ALCOHOL DEHYDROGENASE 1* (*ADH1*) and *PGB1*. Two *ERF-VIIs*, *HYPOXIA-RESPONSIVE ERF 1* (*HRE1*) and *RELATED TO AP2 3* (*RAP2.3*), were also ethylene induced (U2). *CBL-INTERACTING PROTEIN KINASE 25*, recently implicated in root hypoxia tolerance (Tagliani et al., 2020) was also strongly upregulated by ethylene (U1). Similarly, transcripts of *HYPOXIA UNKOWN PROTEIN 54* (AT4G27450) were already enhanced in response to ethylene. Ethylene also enhanced genes associated with water deprivation responses, which is a typical stress during re-oxygenation (Yeung et al., 2019). Apart from ABA biosynthesis and signaling (U1) this included ROS amelioration (U2) consisting of several peroxidases, including *ASCORBATE PEROXIDASE2* (Figure 2E; Supplemental Figure S6). However, several peroxidases were also enriched in the ethylene downregulated cluster D1.

Collectively, this transcriptomic analysis demonstrates that ethylene mediates the majority of DEGs already prior to hypoxia stress and controls processes that include root growth cessation, hypoxia responses, and ROS homeostasis and amelioration.

Downloaded from https://academic.oup.com/plphys/article/190/2/1365/6595039 by Erasmus University Library user on 29 September 2022

Ethylene enhances proteins involved in ROS homeostasis and both mitochondrial and anaerobic respiration

In addition to transcription, changes in translational activity and proteolysis are also considered to be vital for protein homeostasis and therefore stress acclimation responses (Chang et al., 2000; Juntawong et al., 2014; Millar et al., 2019). De novo protein synthesis is dramatically impaired during severe hypoxia (Sachs et al., 1980), and the capacity to produce a newly synthesized set of proteins is essential for hypoxia acclimation (Ellis et al., 1999). Providing mild hypoxia allows de novo protein synthesis and is considered crucial for successful acclimation to severe anoxia (Chang et al., 2000). We therefore profiled the proteome of the root tips after 4 h of pretreatment with ethylene or air, the timepoint at which most ethylene-mediated transcript-level differences were established and the plants would still display strong translation capacity (Figure 2B).

With a cut-off of 2 or more detected peptides for protein recognition, we quantified 6,525 Arabidopsis proteins using isobaric multiplex tandem mass tag (TMT)-based quantitative mass spectrometry (MS) (Supplemental Data, Sheets 8–10). Ethylene enhanced the abundance of 435 proteins and decreased the abundance of 350 proteins (Figure 3A). A GO analysis revealed an enrichment of processes that to some extent mirrored those found in the transcriptome analysis (Figure 3B). This included an upregulation of water deprivation responses, protein folding and anaerobic metabolism, and a downregulation of DNA replication and translation. Additionally, we found an auxin signature, indicating alterations in the root developmental program. GO terms that were unique to the proteomics dataset were associated with the mitochondria, lipid metabolism, and multivesicular bodies. Interestingly, a direct comparison of transcript and protein responses revealed little association (Figure 3C). Many ethylene-regulated proteins did not change at the transcript level, with the important exceptions of PGB1, HYPOXIA RESPONSE UNKNOWN PROTEIN 36 (HUP36), AT1G21400 (THDP-binding superfamily protein), and Nitrate Reductase 1 (Figure 3, C–D). Among upregulated proteins there was only a mild but significant enrichment of genes with a corresponding regulation at the transcript level (odds ratio 95% CI = 1.8–3.2, $P < 0.001$), and this was even less pronounced for downregulated proteins (odds-ratio 95% CI = 1.1–2.0, $P < 0.05$).

Protein levels can be modulated by changes in mRNA stability, translation, and proteolysis. The most differentially ethylene-enriched protein detected was PGB1. We have previously demonstrated that ethylene-enhanced PGB1 levels promote ERFVII protein abundance by limiting NO-dependent proteolysis of these Met_1Cys_2(MC)-initiating ERFVII proteins through the PRT6 N-degron pathway (Gibbs et al., 2014, 2018; Hartman et al., 2019). In the current dataset, 29 other MC-initiating proteins were detected, but none were enriched in response to ethylene (Supplemental Table S1; Supplemental Data, Sheet 11). However, ethylene treatment reduced the abundance of three MC-proteins with unknown biological function (AT5G12850, AT2G10450, and AT2G26470; Supplemental Table S1). A comparison with previously reported proteins upregulated in both the PRT6 N-degron loss-of-function mutants *prt6* and *ate1ate2* showed that at least three proteins (PGB1, HUP54, and AT5G63550) were also induced by ethylene (Supplemental Table S2; Zhang et al., 2015). In general, the proteome profiling results suggest that ethylene regulates protein abundance partially through transcription, but also through yet unidentified changes in translation and proteolysis.

Notable findings among the top 30 most upregulated proteins were PGB1, HUP26, and HUP36 (Figure 3D). PGB1 and HUPs are core hypoxia-responsive genes (Mustroph et al., 2010), typically associated with hypoxia acclimation. Interestingly, they were enhanced in response to ethylene despite the absence of hypoxia. To assess whether this ethylene-enhanced abundance of HUP proteins is beneficial for surviving subsequent hypoxia, we evaluated root tip hypoxia survival in overexpression lines of the three HUPs (-26, -36, and -54) upregulated in the proteomics dataset (Supplemental Figure S7). The results indicated that, compared to wild-type (WT) Col-0, overexpression of *HUP26* and *36*, but not *HUP54* resulted in a higher basal hypoxia tolerance even in the absence of an ethylene pretreatment. Additionally, *HUP36* and *HUP54* overexpression increased ethylene-induced hypoxia tolerance relative to WT (Supplemental Figure S7). This provides support for the involvement of HUP26 and HUP36 in ethylene-mediated hypoxia acclimation of root tips.

Amongst the top induced proteins were also several proteins associated with mitochondrial respiration, located in the mitochondrial electron transport chain (mETC), NITRATE REDUCTASE1 (NR1), and peroxidases (Supplemental Data, Sheet 12). Among the top downregulated proteins were several ribosomal proteins. These findings echoed the GO term enrichment amongst the ethylene-regulated proteins (Figure 3, B and C) and the GO terms identified at the transcript level. In summary, these results reveal that an ethylene treatment quantitatively alters the Arabidopsis root tip proteome and pinpoints modulation of mitochondria, ROS-redox and amelioration, anaerobic metabolism, and translation as key processes that are affected and could aid subsequent hypoxia acclimation.

Ethylene improves antioxidant levels and ROS amelioration during hypoxia and re-oxygenation

Both the transcriptomics and proteomics data suggest that ethylene not only mediates ROS homeostasis and antioxidant activity during the pretreatment but also during subsequent hypoxia and re-oxygenation. As ROS signaling is essential for flooding acclimation, and re-oxygenation is associated with toxic levels of ROS accumulation (Yeung et al., 2019), we explored the role of ethylene in ROS homeostasis. Ethylene affected the transcript and protein abundance of several

Downloaded from https://academic.oup.com/plphys/article/190/2/1365/6595039 by Erasmus University Library user on 29 September 2022

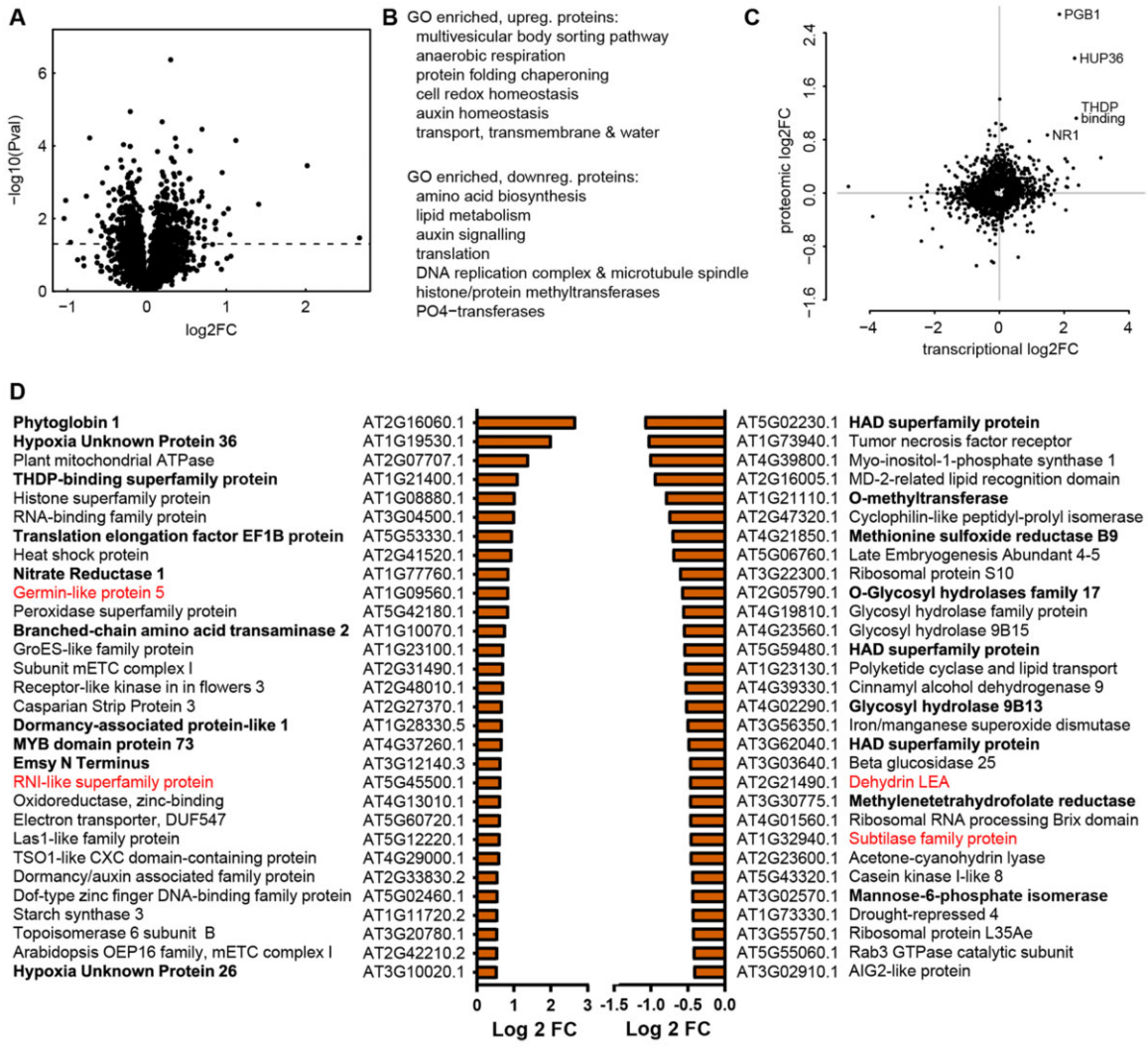

Figure 3 Ethylene treatment modulates the Arabidopsis root tip proteome. A, Volcano plots showing the quantitative change in protein abundance upon 4 h of ethylene treatment (5 $\mu L \cdot L^{-1}$; the pretreatment) and the statistical significance. Dashed line indicates $P = 0.05$. B, Key processes, functions and locations enriched among up and down regulated proteins based on gene ontology (GO) enrichment. Full lists of GO terms are available in the Supplemental Data (Sheet 10). C, Direct comparison of transcriptomic and proteomic response for individual genes. D, The 30 strongest up and down regulated proteins are shown based on fold change. Proteins in bold are also regulated in the corresponding direction at the transcript level. Proteins in red showed an opposite response at the transcript level. All proteins shown are significantly different ($P < 0.05$, Student's t test, $n = 5$).

peroxidases (Figures 2 and 3; Supplemental Figure S6). Considering this and given that the peroxidase-mediated control of hydrogen peroxide (H_2O_2) strongly contributes to cellular antioxidant capacity (Das and Roychoudhury, 2014), we assessed total soluble peroxidase activity in Arabidopsis root tips. We found higher peroxidase activity in the ethylene pretreated samples both during the ethylene pretreatment and subsequent hypoxia and re-oxygenation phase (Figure 4A). The Glutathione–Ascorbic acid (AA) pathway (Foyer and Noctor, 2011) also plays a major role in ROS homeostasis and changes in glutathione and AA are established indicators of changes in cellular redox status. Therefore, we assessed how ethylene modulates the levels of these compounds. No differences were observed in AA content in response to ethylene or subsequent hypoxia and re-oxygenation (Figure 4B). However, our results revealed that ethylene may alter the antioxidant capacity through total glutathione abundance (Figure 4, C and D). After an ethylene pretreatment, both the reduced (GSH) and oxidized glutathione (GSSG) levels increased, and this effect was maintained after 4 h of hypoxia, but not during re-oxygenation (Figure 4, C and D). However, the GSH:GSSG ratio did not change during any of the treatments (Figure 4, C–E). These results are consistent with the report that ethylene insensitive mutants are impaired in glutathione biosynthesis, but not in AA production during abiotic stress (Yoshida et al., 2009). Together, these results reveal that ethylene may alter ROS homeostasis through changes in at least peroxidase activity and glutathione content.

Downloaded from https://academic.oup.com/plphys/article/190/2/1365/6595039 by Erasmus University Library user on 29 September 2022

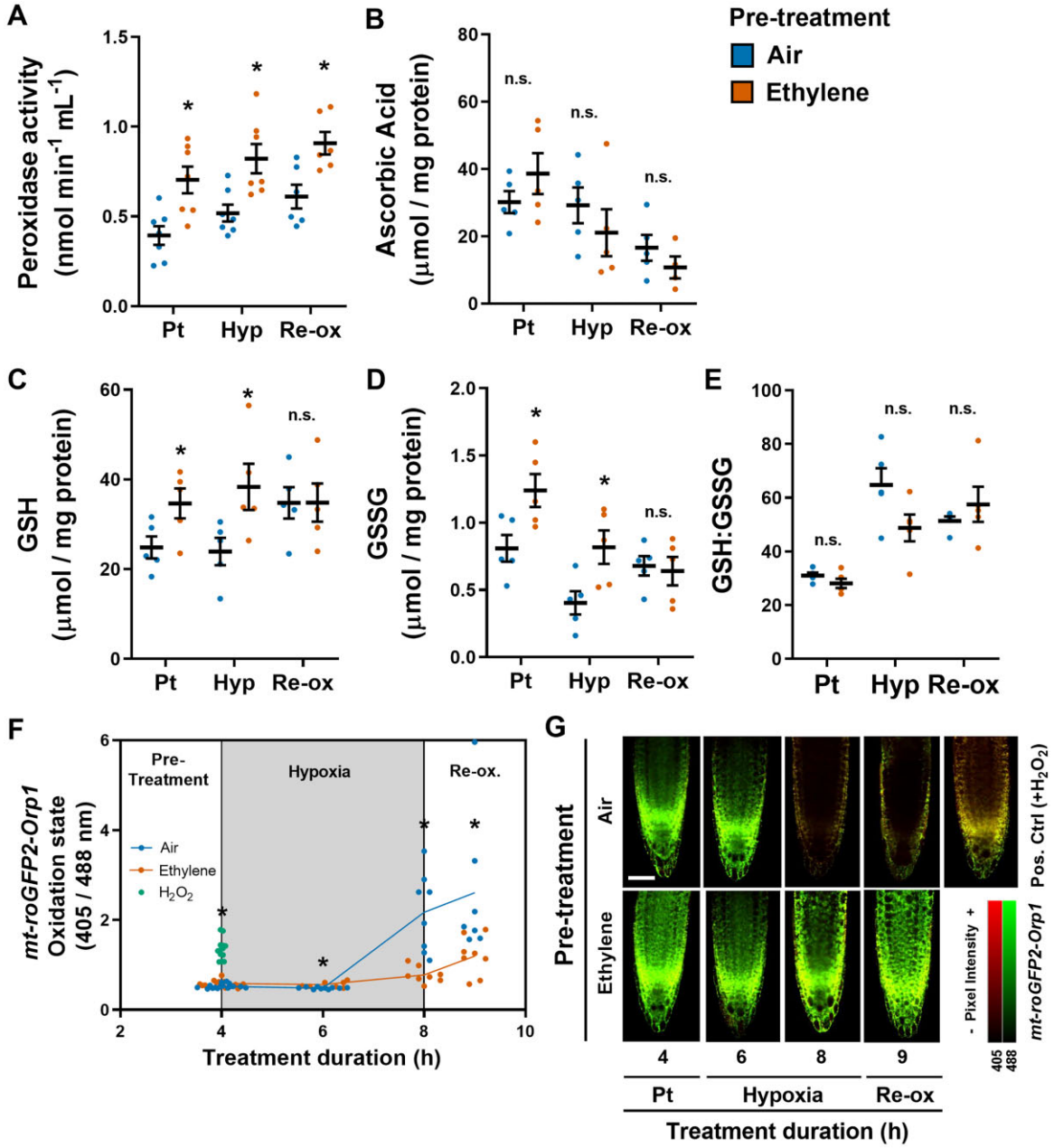

Figure 4 Ethylene mediates antioxidant capacity and ROS homeostasis after pretreatment and subsequent hypoxia and re-oxygenation. A–E, Peroxidase activity (A), AA (B), reduced glutathione (GSH, C), oxidized glutathione (GSSG, D), and the GSH:GSSG ratio (E) in 5-day-old Arabidopsis Col-0 root tips after 4 h of air or ~5 µL·L^{-1} ethylene pretreatment (Pt) followed by 4 h of hypoxia (Hyp) and 1 h of re-oxygenation (Re-ox) (Asterisks indicate significant differences between air and ethylene per time point (*$P < 0.05$, Student's t test, n = 5–6 plates of approximately 600 seedling root tips). Dots indicate a single plate of seedling root tips, error bars represent [AQ]SEM (A–E). F and G, Quantification (F) and representative overlay images (G) of the oxidation state of mitochondrial targeted reduction-oxidation sensitive (ro)GFP2-Orp1 in Arabidopsis root tips after 4 h of pretreatment with air or ~5 µL·L^{-1} ethylene followed by 2 and 4 h of hypoxia and 1 h of re-oxygenation. The oxidation state of roGFP2-Orp1 is calculated from 405/488 nm excitation ratios, where a higher oxidation rate corresponds to elevated H_2O_2 in mitochondrial matrix (Nietzel et al., 2019). A positive control was included at the 4 h timepoint by adding 20-mM H_2O_2 to the root tip, 30 min prior to imaging (green). Scale bar = 50 µm (G). Asterisks indicate significant differences between air and ethylene per time point (*$P < 0.05$, Student's t test, n = 7–16 root tips).

Next, we assessed if ethylene pretreatment altered ROS levels during subsequent hypoxia and re-oxygenation. For this, we used two different methods to visualize H_2O_2 in Arabidopsis root tips. First, we used the transgenic H_2O_2-reporter line reduction–oxidation sensitive Green Fluorescent Protein-Oxidant Receptor Peroxidase1 (roGFP2-Orp1) which allows *in vivo* visualization and quantification of H_2O_2 in specific organelles at a subcellular level (Nietzel et al., 2019). Since a large portion of ROS is formed inside mitochondria through excessive electron flow through the electron

Downloaded from https://academic.oup.com/plphys/article/190/2/1365/6595039 by Erasmus University Library user on 29 September 2022

transport chain (ETC) (Vanlerberghe, 2013) and ethylene led to differences in several proteins located in the mETC (Figure 3, B and C), we decided to study the mitochondrion-specific (mt-) roGFP2-Orp1(Nietzel et al., 2019). Application of H_2O_2 to root tips prior to imaging, functioned as a positive control and showed an enhanced roGFP2-Orp1 oxidation state, indicative of higher H_2O_2 levels (Figure 4, F and G). Ethylene pretreatment alone slightly increased mitochondrial H_2O_2 levels in Arabidopsis root tips (Figure 4, F and G). After both 4 h of hypoxia and 1 h of re-oxygenation, H_2O_2 levels increased drastically in air pretreated root tips. However, excessive ROS formation observed in the mitochondria was strongly limited after an ethylene pretreatment. As a second approach to visualize H_2O_2 we used 3,3′-Diaminobenzidine (DAB) staining. Again, an ethylene pretreatment limited root tip H_2O_2 accumulation during subsequent hypoxia and re-oxygenation timepoints (Supplemental Figure S8). Collectively, these results suggest that ethylene is essential to boost antioxidant capacity and limit the excessive ROS formation during subsequent hypoxia and re-oxygenation in Arabidopsis root tips.

Ethylene improves oxidative stress tolerance

Our results show that a large proportion of Arabidopsis root tips loses cell integrity during re-oxygenation (Figure 1, B and C; Supplemental Figure S1, B and C). We, therefore, wondered whether the pronounced increase in H_2O_2 during hypoxia and re-oxygenation (Figure 4, F and G) leads to oxidative stress and subsequent reduced survival in these root tips. Or conversely, that impaired cell integrity leads to elevated H_2O_2 levels as ROS homeostasis can no longer be maintained. To untangle this question, we first examined whether ethylene-mediated ROS amelioration contributes to enhanced hypoxia survival by applying the pharmaceutical ROS scavenger potassium iodide (KI). Indeed, like an ethylene pretreatment, the application of either 1- or 5-mM KI strongly boosted hypoxia root tip survival (Figure 5A). While these results demonstrate that improved ROS amelioration contributes to hypoxia survival, it does not reveal a direct effect of ethylene on enhanced oxidative stress tolerance. Therefore, we tested whether an ethylene pretreatment could improve oxidative stress survival independent of hypoxia stress. Accordingly, small droplets of H_2O_2 were applied directly to the root tips after an air or ethylene pretreatment to induce oxidative stress. Application of 6 mM H_2O_2 strongly reduced root tip survival, but this impaired survival could be rescued by an ethylene pretreatment (Figure 5B). Similar to ethylene-enhanced hypoxia tolerance (Hartman et al., 2019), this ethylene-mediated ROS tolerance was dependent on the established ethylene-signaling EIN3/EIL1 transcription factor complex (Alonso et al., 2003), as both the *ein2-5* and *ein3-1eil1-1* double mutants no longer benefited from an ethylene pretreatment (Figure 5B). Disruption of ethylene detection, through the receptor mutant line *etr1-1* also diminished ethylene-mediated enhanced tolerance to ROS (Figure 5C). Conversely, enhanced endogenous ethylene production in the *eto1eol1eol2* triple mutant improved survival to H_2O_2 application compared to the WT Col-0 (Christians et al., 2009). Taken together, these results suggest that ethylene-mediated ROS amelioration contributes to hypoxia tolerance in Arabidopsis.

We showed previously that ethylene-mediated hypoxia tolerance is controlled by impairment of the PRT6 N-degron pathway through PGB1-mediated NO depletion and subsequent enhanced stability of RAP2.2 and RAP2.12 (Hartman et al., 2019). In the current proteomics data set, PGB1 was the most enriched protein in response to ethylene treatment (Figure 3C). To evaluate whether this mechanism also contributes to ethylene-mediated ROS amelioration, we first assessed root tip survival following H_2O_2 application in a *PGB1* knockdown (Hartman et al., 2019) and overexpression line. Ethylene still increased H_2O_2 survival in *pgb1-1*, but to a lesser extent than the WT Col-0 (Figure 5D). Moreover, *35S:PGB1* exhibited enhanced oxidative stress survival without an ethylene pretreatment, suggesting that PGB1 is at least partially involved in ethylene-mediated oxidative stress tolerance. We also examined root tip H_2O_2 survival in the *prt6-1* mutant in which proteins with the corresponding N-recognin are stabilized, with a subsequent effect on downstream targets and hypoxia tolerance (Holman et al., 2009; Riber et al., 2015; Zhang et al., 2015).The *prt6-1* root tips showed a strong increase in oxidative stress survival compared to Col-0, such that *prt6-1* seems constitutively ethylene primed (Figure 5E).

NO scavenging by ethylene-induced PGB1 limits ERFVII RAP2.2 and RAP2.12 turnover via the PRT6 branch of the N-degron pathway, aiding hypoxia acclimation (Hartman et al., 2019). We next tested the double null mutant *rap2.2 rap2.12* for ethylene-induced ROS tolerance. Basal levels in H_2O_2 tolerance were slightly reduced, but ethylene-enhanced tolerance was unaffected in the double mutant (Figure 5F) relative to the WT background. Given that *rap2.2 rap2.12* has reduced hypoxia tolerance (Gasch et al., 2016; Hartman et al., 2019), but did not impact ethylene-mediated oxidative-stress tolerance during normoxia (Figure 5F), we tested whether this line may be altered in ROS homeostasis under actual hypoxia. For this, we used DAB staining to visualize H_2O_2 in root tips during hypoxia and re-oxygenation (Figure 5G). Indeed, in the WT, ethylene increased the number of root tips free of DAB stain and this ethylene benefit was absent in the *rap2.2rap2.12* double mutant. The oxidative stress tolerance assay and ROS profiling under hypoxia suggest that RAP2.2 and RAP2.12 may not directly aid ethylene-induced ROS scavenging, but rather that hypoxia acclimation and associated viability mediated by these ERFVIIs (Hartman et al., 2019) is crucial to mount a successful response to re-oxygenation. This contrasts with the results for *PGB1* and *PRT6*, suggesting that these proteins, in addition to their role in ERFVII stabilization also directly play a key role in ethylene-mediated ROS scavenging.

Downloaded from https://academic.oup.com/plphys/article/190/2/1365/6595039 by Erasmus University Library user on 29 September 2022

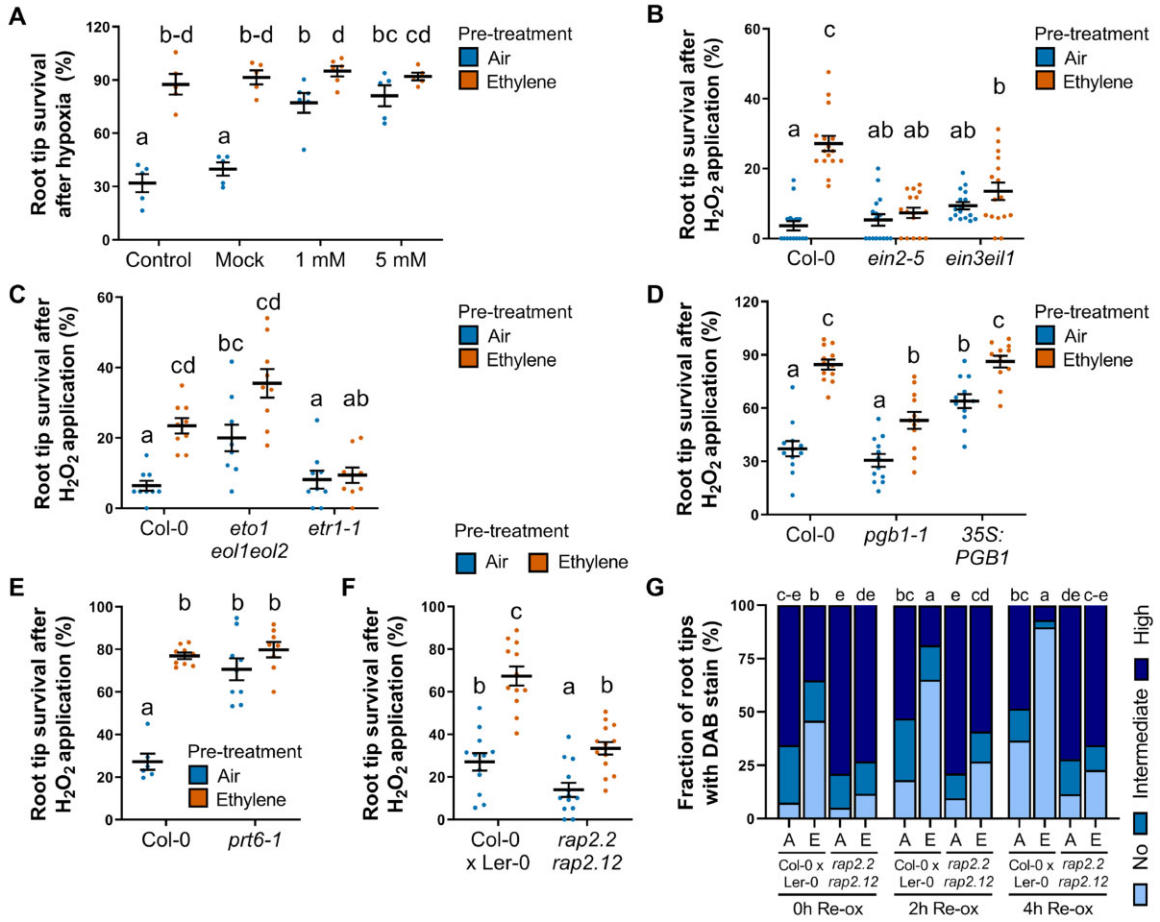

Figure 5 Ethylene improves oxidative stress survival. A, Root tip survival of 4-day-old Arabidopsis (Col-0) seedlings after 4 h of air or ~5 μL·L^{-1} ethylene treatment in combination with application of mock or 1-mM or 5-mM ROS scavenger KI, followed by 4 h of hypoxia and 3 days of recovery (n = 5 plates containing approximately 46 seedlings). B–F, Root tip survival of (B) Col-0 and ethylene insensitive mutants *ein2-5* and *ein3eil1*, (C) Col-0, ethylene enhanced biosynthesis mutant *eto1eol1eol2* and receptor mutant *etr1-1*, (D) Col-0, *pgb1-1* and *35S:PGB1*, (E) Col-0, N-degron mutant *prt6-1* (Col-0 background) and a (F) Col-0 x Ler-0 cross and ERFVII double mutant *rap2.2rap2.12* (Col-0 x Ler-0 background) after 4 h of air or ~5 μL·L^{-1} ethylene treatment followed by application of 5 μL of H_2O_2 (6 mM) on each single root tip and 3 days of recovery. Statistically similar groups are indicated using the same letter (n = 5–16 rows containing approximately 23 seedlings). G, Proportion of WT (Col-0 x Ler-0 background) or ERFVII double mutant *rap2.2rap2.12* (Col-0 x Ler-0 background) root tips showing H_2O_2 (DAB) staining after air or ~5 μL·L^{-1} ethylene treatment followed by 4 h of hypoxia and 2 h of re-oxygenation. Statistically similar groups are indicated per timepoint using the same letter (n = 146–180 root tips). Dots indicate a single row/plate of seedlings, error bars represent SEM (A–F). For (A–G) the letters indicate significantly indistinguishable groups ($P < 0.05$) based on Tukey's [AQ]HSD following a generalized linear model with binomial link function (GLM-binomial). The effect of ethylene on ROS tolerance or DAB staining was tested for with an interaction term in a GLM-binomial with a genotype (WT and mutant) and pretreatment (ethylene-control) effect. Interaction terms for H_2O_2 tolerance were statistically significant for *ein2-5* (P = 2e-4), *ein3/eil1* (P = 1e-5), *etr1-1* (P = 0.04), *pgb1* (P = 1e-4), *35S:PGB1* (P = 0.002), *prt6-1* (P = 3e-8), but not for *eto1eol1eol2* (P = 0.1541), and *rap2.12/2.2* (P = 0.21). DAB staining interaction terms were 0 h (P = 0.01), 2 h (P = 0.04), 4 h (P = 9e-6).

Ethylene rapidly limits root growth, which may contribute to enhanced hypoxia tolerance

The transcriptomic analysis revealed both established and previously unknown ethylene-driven gene clusters and genes that are indicative of ethylene-mediated root growth cessation. Indeed, ethylene is a known inhibitor of root growth and development (Le et al., 2001). We hypothesized that energy and resources saved by inhibition of development could, in addition to ROS amelioration, aid in hypoxia tolerance. We first investigated whether the duration of the ethylene pretreatment used was sufficient to inhibit root growth in our experimental system. A significant reduction in root growth (measured as an increase in primary root length) was observed already after 1 h of ethylene treatment compared to the air control. This root growth cessation was maintained for the entirety of the 4 h ethylene pretreatment (Supplemental Figure S9).

To separate the effects of growth cessation from other ethylene-mediated tolerance mechanisms we employed the *asa1-1* mutant. ASA1 is a direct target of ERF1 and encodes a rate-limiting step of tryptophan biosynthesis, required for auxin biosynthesis. Ethylene-mediated auxin

Downloaded from https://academic.oup.com/plphys/article/190/2/1365/6595039 by Erasmus University Library user on 29 September 2022

accumulation via ASA1 leads to inhibition of primary root growth, but this is reported to be absent in *asa1-1* (Mao et al., 2016). The *asa1-1* mutant thus would allow us to apply ethylene and elicit the entire ethylene signaling pathway, but not inhibit root growth. However, in our experimental set-up *asa1-1* had faster root growth rates compared to WT, under both control and ethylene conditions. The *asa-1* mutation also did not impact ethylene-mediated root growth inhibition (Figure 6A). Nonetheless, the subsequent increased root growth in *asa1-1*, lead to reduced root tip survival under hypoxia compared to WT, in both control and ethylene pretreatment. Furthermore, similar to root growth inhibition, the positive effects of ethylene on survival were maintained in *asa1-1* (Figure 6B). The *asa1-1* mutant, with altered growth rates and altered tolerance, resulted in a continuum of growth-tolerance values with a strong relationship that associated low growth with high survival (Figure 6C).

Manipulation of ASA1 function led to changes in growth independent of ethylene and revealed the relationship between growth and tolerance. To further explore manipulation of ethylene-mediated growth inhibition we utilized the *aux1-22* mutant (Swarup et al., 2007). In the auxin signaling *aux1-22* mutant, ethylene treatment still leads to known ethylene-responsive gene induction, but no longer to auxin-responsive gene induction and subsequent root growth cessation by ethylene in the epidermis (Růžička et al., 2007; Swarup et al., 2007; Vaseva et al., 2018). In our setup ethylene did cause a significant reduction in *aux1-22* root growth, but this inhibition of root growth was considerably less than in Col-0 (Figure 6D). This trend was mirrored in root hypoxia survival. While ethylene still enhanced *aux1-22* hypoxia survival, the effect was significantly reduced relative to the WT (Figure 6E). Subsequently, also with *aux1-22*, we found a clear association between low root growth and high survival (Figure 6F). Overall, we demonstrate that

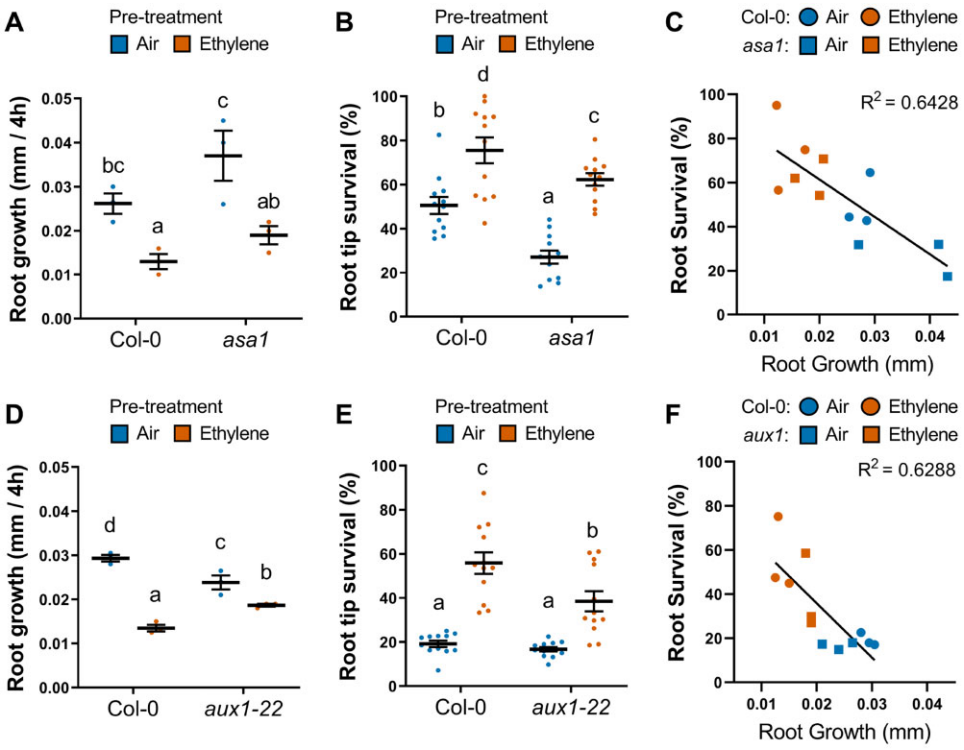

Figure 6 Ethylene-mediated root growth cessation contributes to enhanced hypoxia survival. A, Root growth (increase in root length) of 4-day old Col-0 and *asa1-1* during 4 h of air or ~5 μL·L^{-1} ethylene treatment compared to root length at *t* = 0. Data, combined from three experiments, are the median growth rate of single plate of 46 seedlings (*N* = 3 plates). Interaction *P*-value is 0.23 (two-way ANOVA). B, Root tip survival of 4-day-old Col-0 and *asa1-1* seedlings after 4 h of air or ~5 μL·L^{-1} ethylene followed by 4 h of hypoxia and 3 day of recovery. Combined data from three experiments is shown (*n* = 12 plates containing approximately 46 seedlings). Interaction *P*-value is 0.05 (GLM–binomial). C, Pearson correlation between growth and survival. Mean results of three independent experiments are shown. D, Root growth (increase in root length) of 4-day-old Col-0 and *aux1-22* during 4 h of air or ~5 μL·L^{-1} ethylene treatment compared to root length at *t* = 0. Data, combined from three experiments, are the median growth rate of single plate of 46 seedlings (*N* = 3 plates). Interaction *P*-value is 4e-4 (two-way [AQ]ANOVA). E, Root tip survival of 4-day-old Col-0 and *aux1-22* seedlings after 4 h of air or ~5 μL·L^{-1} ethylene followed by 3.5 h of hypoxia and 3 days of recovery (*n* = 12 plates containing approximately 23 seedlings, combined data from three experiments is shown). Interaction *P*-value is 0.01 (GLM and binomial) (F) Pearson correlation between growth and survival. Mean results of three independent experiments are shown. Shared letters indicate significantly indistinguishable groups ($P < 0.05$) based on Tukey's HSD following an ANOVA (growth data) or a generalized linear model with binomial link function (GLM–binomial, survival data). Interaction terms were assessed with a GLM–binomial or two-way ANOVA with a genotype (WT and mutant) and pretreatment (ethylene-control) effect.

Downloaded from https://academic.oup.com/plphys/article/190/2/1365/6595039 by Erasmus University Library user on 29 September 2022

growth manipulation, either dependent or independent from ethylene, leads to altered hypoxia tolerance. This suggests that growth cessation contributes to ethylene-mediated tolerance to hypoxia.

Discussion

In this study, we looked for potential genes, proteins, and processes that contribute to ethylene-mediated improved hypoxia survival of Arabidopsis root tips. Our results show that ethylene increases both hypoxia and re-oxygenation survival. The data suggest that ethylene may contribute to enhanced tolerance through multiple processes including enhanced hypoxia responses, ROS amelioration responses, and reduction of root growth (Figure 7).

Ethylene has an important role as a distress signal during various environmental stresses. This can be of critical importance for tolerance and has been reported for hypoxia (reviewed in Hartman et al., 2021), salt (Peng et al., 2014), drought (Skirycz et al., 2011), freezing (Wu et al., 2008), and soil compaction stress (Pandey et al., 2021). In our study, the major ethylene-mediated transcriptomic changes occurred during the pretreatment, without any additional changes upon subsequent hypoxia. This suggests that ethylene-mediated changes occurring before the onset of hypoxia contribute to increased tolerance during hypoxia and re-oxygenation. Indeed, in general, translation and protein synthesis are typically strongly restricted during severe hypoxia stress (Chang et al., 2000; Juntawong et al., 2014). Accordingly, an acclimation period prior to the onset of severe stress can improve subsequent stress tolerance. We propose that for flooding, ethylene could fulfill such a role because inducing protective responses may be energetically challenging to achieve under severe hypoxic stress. Both the transcriptomics and proteomics results suggest that ethylene may also control a general downregulation of translation and growth, which could be adaptive to quickly limit energy expenditure. Ethylene-mediated repression of growth responses and translation could be of great importance to improve survival chances during hypoxia.

Ethylene partially restrains root growth by stimulating auxin synthesis and transport (Růžička et al., 2007; Swarup et al., 2007; Mao et al., 2016). Our results suggest that this ethylene-induced and AUX1-dependent auxin signaling in the root could contribute to subsequent hypoxia survival, as *aux1-22* was more sensitive to hypoxia after ethylene treatment compared to the WT (Figure 6E). While transcriptome profiling identified the classical genes involved in ethylene-mediated root growth, it also identified many growth regulators that were not previously associated with ethylene, such as *UPBEAT1*, *MYB30*, and *PLETHORA1/2* (Aida et al., 2004; Tsukagoshi et al., 2010; Mabuchi et al., 2018). Currently, it is unclear whether these are under direct control of ethylene signaling or act indirectly via ethylene-mediated auxin and ROS homeostasis. It also remains to be investigated whether their regulation by ethylene contributes to root growth cessation and hypoxia tolerance. Ethylene-mediated root growth suppression seems universal in the plant kingdom (Visser and Pierik, 2007). That the *asa1* and *aux1-22* root tips, which have altered growth rates either with or without ethylene, have altered hypoxia tolerance or capacity to

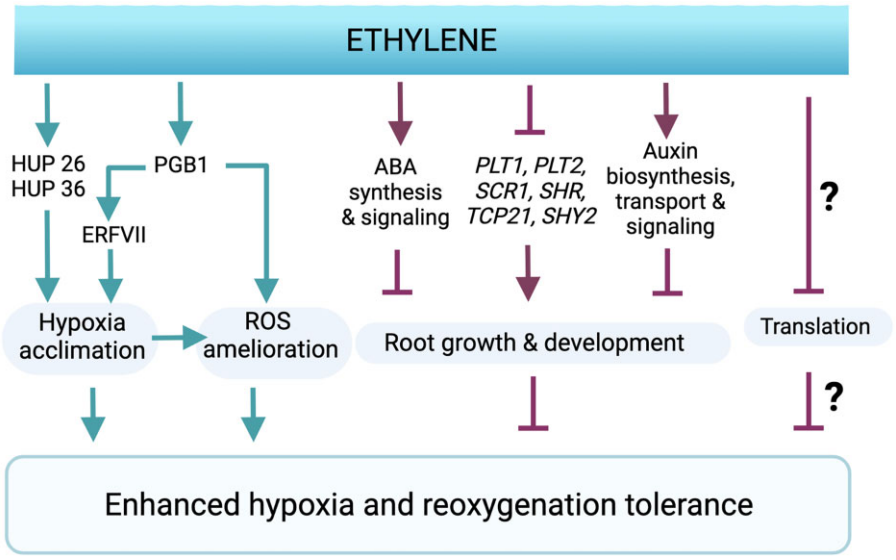

Figure 7 Ethylene modulates a range of acclimation responses to sustain hypoxia and re-oxygenation damage. Proposed model of how ethylene contributes to sustain hypoxia and re-oxygenation stress. Ethylene accumulation during flooding prepares cells for impending severe hypoxia via various means: enhanced accumulation of PGB1 (which scavenges NO and stabilizes ERFVIIs) and [AQ]HUP proteins required for hypoxia acclimation; ROS homeostasis is also mediated by PGB1, either directly via yet unknown mechanisms or indirectly because of ERFVII stabilization and consequent cellular hypoxia protection; Repression of energetically expensive processes of translation and root growth and development. The latter likely involves transcriptional regulation of root developmental regulators and hormone activity. Together the enhanced hypoxia response, ROS amelioration and root growth cessation by ethylene contribute to reduce hypoxia and re-oxygenation stress and improve hypoxia survival. Red and green pathways indicate processes reducing or enhancing hypoxia and re-oxygenation tolerance, respectively. Created with BioRender.com.

Downloaded from https://academic.oup.com/plphys/article/190/2/1365/6595039 by Erasmus University Library user on 29 September 2022

prime suggests that this growth suppression mediated by early ethylene is a critical strategy for flooding-induced hypoxia survival. The functional consequences of ethylene-mediated growth repression on hypoxia tolerance could therefore be a promising avenue for future research and for the development of flood-tolerant crop cultivars.

In addition to root growth cessation and translation, we identified an overrepresentation of genes and proteins related to hypoxia and flooding responses (Figures 2, E and 3). The hypoxia response GO term was enriched for ethylene-independent genes as well as for ethylene-enhanced genes, suggesting that there is both an ethylene-dependent and independent hypoxia response in Arabidopsis root tips. Within the ethylene-mediated hypoxia response cluster, there were many genes well-known for their role in hypoxia acclimation, such as *PGB1*, *HRE1/2*, *ADH1*, *PDC1*, and several *HUPs* (Licausi et al., 2010; Mustroph et al., 2010; Hebelstrup et al., 2012; Mithran et al., 2014; Hartman et al., 2019). Moreover, the proteomics results revealed that ethylene also enhances the protein abundance of PGB1 and HUP36, HUP26, and HUP54. In previous studies, constitutive overexpression of single *HUPs* resulted in altered flooding or hypoxia tolerance only in some lines and these effects were variable (Mustroph et al., 2010; Lee et al., 2011). We observed a minor benefit in hypoxia tolerance in *HUP36*, *HUP26*, and *HUP54* overexpressors (Supplemental Figure S7). It is likely that a collection of hypoxia-responsive genes needs to be activated in concert for achieving substantial beneficial effects for survival. Our results further emphasize that ethylene can promote a subset of hypoxia-responsive genes and proteins prior to the onset of hypoxia to subsequently promote hypoxia survival (Figure 6).

Finally, we identified an overrepresentation of ethylene-enriched genes and proteins related to ROS homeostasis and amelioration (Figures 2, E and 3, A). Modulation of ROS homeostasis and the induction of ROS signaling has previously been shown to control plant growth and stress responses (Mittler, 2017; Sasidharan et al., 2018). Ethylene-modulation of ROS signaling also controls several flood-adaptive anatomical and growth responses in species such as rice and maize, such as the formation of aerenchyma and adventitious roots (Steffens et al., 2012; Yamauchi et al., 2014; Ni et al., 2019; Qi et al., 2019). In addition, ROS signaling is essential to regulate the transcriptional hypoxia response and mutants showing abnormal ROS signaling are more hypoxia and flood sensitive (Pucciariello et al., 2012; Gonzali et al., 2015; Yang and Hong, 2015; Sasidharan et al., 2018; Huang et al., 2022). Recent reports demonstrate that ROS signaling is partially dependent on ethylene signaling to transcriptionally induce the hypoxia genes *ADH1* and *HRE1* (Hong et al., 2020). However, ethylene-controlled ROS amelioration during flooding, hypoxia, and re-oxygenation stress has hardly been investigated (Yeung et al., 2019; Hartman et al., 2021). Prior research has shown that ethylene-insensitive Arabidopsis mutants experience increased damage during re-oxygenation (Tsai et al., 2014). Accordingly, we show that an ethylene pretreatment improves root tip survival during hypoxia and re-oxygenation stress (Figure 1; Supplemental Figure S1). These results coincide with the observation that hypoxia and re-oxygenation lead to excessive ROS formation in root tips and that ethylene strongly limits this accumulation (Figure 4, D and E). Importantly, we demonstrate that enhanced ROS scavenging during and after hypoxia is essential to improve hypoxia survival (Figure 5A), and that ethylene treatment markedly improves the survival of root tips subjected to oxidative stress (Figure 5, B–F). Collectively, these data strongly suggest that ethylene facilitates hypoxia and re-oxygenation stress survival through enhanced ROS amelioration (Figure 4).

How ethylene exactly promotes ROS homeostasis to facilitate hypoxia tolerance remains unclear. However, we found that ethylene enhanced transcript levels of genes involved in the Glutathione–AA pathway (Foyer and Noctor, 2011), and changed the abundance of several peroxidases. We also observed that an ethylene treatment alone led to an increase in the total glutathione pool and peroxidase activity which was maintained during subsequent hypoxia (Figure 4, A and C). These observations are consistent with reports showing that ethylene promotes peroxidase activity (Gahagan et al., 1968; Mehlhorn, 1990) and glutathione production (Yoshida et al., 2009). Since both glutathione and peroxidases are essential to buffer cellular antioxidant capacity (Gill et al., 2013; Das and Roychoudhury, 2014), it would be interesting to identify whether these changes are required for ethylene-mediated oxidative stress and hypoxia tolerance.

We previously demonstrated that ethylene-induced PGB1 is essential to prevent NO-dependent ERFVII proteolysis and confer subsequent hypoxia tolerance (Hartman et al., 2019). Here we show that PGB1 and the PRT6 pathway are also partially involved in ethylene-mediated ROS tolerance (Figure 5, D–G). Notably, enhanced oxidative stress tolerance mediated by ethylene does not require ERFVIIs (Figure 5F). However, ERFVII loss of function did affect the ethylene-mediated ROS amelioration during and after hypoxia (Figure 5G). A similar effect was found in ERFVII single mutants that responded poorly to osmotic stress but were unaffected by H_2O_2 treatment (Papdi et al., 2015). We suggest that ERFVIIs are key for hypoxia acclimation, leading to improved viability and therefore indirectly improve the capacity of the cellular machinery for ROS scavenging and homeostasis during re-oxygenation stress.

In contrast, PGB1 and PRT6 function are important and likely have a direct effect on ethylene-improved antioxidant capacity. Previous research has linked ethylene, PGB1 and PRT6 to reduced ROS levels during multiple abiotic stresses, including flooding and hypoxia stress. Indeed, overexpression of PGB1 putative orthologs in maize (*Zea mays*) and soybean (*Glycine max*) led to elevated antioxidant levels, reduced ROS accumulation, enhanced waterlogging, and drought stress tolerance and was linked PGB's NO scavenging capacity (Youssef et al., 2016; Hammond et al., 2020; Mira et al., 2021). In barley, a *prt6* knockout also exhibited

Downloaded from https://academic.oup.com/plphys/article/190/2/1365/6595039 by Erasmus University Library user on 29 September 2022

improved ROS tolerance and increased performance under abiotic stress (Vicente et al., 2017). Additionally, proteomic analysis of *prt6* Arabidopsis roots showcases elevated expression of three peroxidases and hemoglobin (Zhang et al., 2015), potentially driving the high ROS tolerance observed in *prt6*. Finally, ethylene plays a critical role in ROS amelioration during abiotic stress responses (Wu et al., 2008; Peng et al., 2014; Tsai et al., 2014), and antioxidant activity is a crucial driver for enhanced abiotic stress tolerance (Arbona et al., 2008; Fukao et al., 2011; Yeung et al., 2018). Collectively, these results suggest that ethylene-mediated ROS amelioration could be an important general trait for abiotic stress-resilient crop breeding and identifies PGBs and PRT6 as potential regulatory targets.

Acute hypoxia as a result of flooding places a heavy burden on plant cells because energy and carbohydrate generation are strongly impaired while these are required to mount adaptive responses and sustain the accumulation of highly damaging ROS. We show the early flooding signal ethylene improves hypoxia survival by regulating a range of processes that facilitate hypoxia acclimation and prevent posthypoxic injury. These ethylene-controlled processes modulated at the transcript and protein level include hypoxia responses, ROS metabolism, growth cessation, and possibly the downregulation of translation, and leads to subsequent enhanced ROS amelioration and hypoxia survival (Figure 7). Finally, we show that ethylene improves oxidative stress survival and propose that this process is pivotal for how ethylene confers hypoxia tolerance in plants.

Materials and methods

Plant material and growth conditions

Arabidopsis thaliana WT lines Col-0, Col-0 × Ler-0 and null mutants *ein2-5*, *ein3-1eil1-1*, *PRT6* defect *prt6-1* (SAIL 1278_H11), *PGB1* knockdown *pgb1-1* (ï»¿SALK_058388), and over-expression line *35S::PGB1*, ERFVII double mutant *rap2.2-rap2.12* (Col-0 × Ler-0 background) were previously described (Hartman et al., 2019), and sterilized for 3 h in a mixture of bleach (30 mL) and concentrated hydrochloric acid (1.5 mL; Sigma-Aldrich, St. Louis, MO, USA). The *pgb1-1* mutant lacks ethylene-induced *PGB1* expression and lower hypoxia-induced *PGB1* expression (relative to WT; Hartman et al., 2019). The ethylene receptor and enhanced biosynthesis mutants *etr1-1* and *eto1eol1eol2* were previously described (Bleecker et al., 1988; Christians et al., 2009). Seeds were sown on sterile, square petri dishes (120 × 120 × 17 mm; Greiner Bio One Frickenhausen, Germany) on 1% w/v plant agar (25 mL, Duchefa Biochemie B.V., Haarlem, The Netherlands; P1001) supplemented with 1/4 Murashige and Skoog (MS; Duchefa Biochemie B.V.; M0245). Forty-six seeds were sown in two rows per plate and plates were sealed with Leucopore tape (12.5 mm; Duchefa Biochemie B.V., L3302). After 4 days of stratification at 4°C in the dark, plates were placed vertically in climate-controlled growth chambers with a short-day photoperiod (daytime: 9–17 h, light intensity: ~120 $\mu mol \cdot m^{-2} \cdot s^{-1}$, humidity: 70%, temperature: 21°C daytime and 18°C nighttime). For recovery, plates were kept in the dark after hypoxia treatment and then moved back to the same short-day growth conditions when the light was switched off in the climate chamber at the end of the day.

Ethylene and hypoxia treatment conditions

For ethylene treatments, seedlings grown on square plates with lids removed were placed vertically inside closed glass desiccators injected with specific ethylene concentrations (light intensity within desiccators: ~5 $\mu mol \cdot m^{-2} \cdot s^{-1}$, room temperature). Seedlings placed in glass desiccators without ethylene were used as control. Commercially purchased gaseous ethylene was diluted to desired concentrations and injected into glass desiccators. After 30 min, gas samples were taken from the desiccators to confirm the ethylene concentration by gas chromatography (Syntech Spectras GC955). For hypoxia treatments, seedlings grown on square plates with lids removed were placed vertically inside closed glass desiccators, which was flushed with gaseous nitrogen at a rate of 2 $L \cdot min^{-1}$ in the dark (typically reaching 0.00% O_2 after 40–50 min of treatment, see Hartman et al., 2019). Seedlings placed in desiccators in which air was flushed at a similar rate were used as control.

H_2O_2 treatments

H_2O_2 (30% w/w, Merck KGaA) was diluted into 1/4 MS to achieve desired concentrations and 5 µL of H_2O_2 solution was applied to each root tip in the dark. Plates were kept horizontal for 15 min to allow the solution to be absorbed by the root tips.

EB staining for cell viability and visualization

For each treatment per replicate, around 20 seedlings were randomly taken from the plates for EB staining of cell integrity at desired time points during hypoxia and subsequent re-oxygenation. Seedlings were incubated in 0.25% w/v aqueous EB solution for 15 min in the dark (room temperature), then washed 3 times with Milli-Q (MQ) water to remove excess dye. Olympus BX50WI was used for visualization and images were taken under 10× objective lens.

Root tip survival and growth quantification and data analysis

Primary root tip survival was scored according to root tip re-growth after 3 days of recovery following hypoxia treatment (Hartman et al., 2019). Survival rate was calculated as the percentage of seedlings that showed root tip re-growth out of the 23 seedlings per row grown vertically on an agar plate. Root tip growth was measured using ImageJ software.

Microarray sample preparation and analysis

Samples were harvested at desired time-points (Figure 2A) and snap frozen in liquid N_2 immediately. Total RNA was isolated using the RNeasy mini kit (Qiagen, Germany). Micro-array was performed commercially by Macrogen (Seoul, South Korea). RNA purity and integrity were evaluated by ND-1000 Spectrophotometer (NanoDrop,

Downloaded from https://academic.oup.com/plphys/article/190/2/1365/6595039 by Erasmus University Library user on 29 September 2022

Wilmington, NC, USA), Agilent 2100 Bioanalyzer (Agilent Technologies, Palo Alto, CA, USA). RNA labeling and hybridization were performed by using the Agilent One-Color Microarray-Based Gene Expression Analysis protocol (Agilent Technology; V 6.5, 2010). Briefly, RNA was linearly amplified and labeled with Cy3-dCTP, purified using the RNeasy mini Kit, and then measured using NanoDrop ND-1000. About 1,650 ng of labeled cRNA was fragmented by adding 11 μL 10 × blocking agent and 2.2 μL of 25 × fragmentation buffer and subsequently heated to 60°C for 30 min. Finally, 55 μL 2 × GE hybridization buffer was added to dilute the labeled cRNA. An aliquot of 100 μL of hybridization solution was dispensed into the gasket slide and assembled to the Agilent SurePrint HD Arabidopsis GE 4X44K Microarrays (Agilent). Slides were incubated for 17 h at 65°C in an Agilent hybridization oven, then washed at room temperature using the Agilent One-Color Microarray-Based Gene Expression Analysis protocol (Agilent Technology; V 6.5, 2010). The hybridized array was immediately scanned with an Agilent Microarray Scanner D (Agilent Technologies, Inc.) Results were extracted using Agilent Feature Extraction software version 11.0 (Agilent Technologies) and can be found in ArrayExpress under accession number E-MTAB-11231 (https://www.ebi.ac.uk/arrayexpress/experiments/E-MTAB-11231) (see also Supplemental Data Sets 2–7). Additionally, the transcript and protein abundance changes in response to ethylene can also be found in a shiny-app (https://utrecht-university.shinyapps.io/Liu2022/).

Gene expression analysis

For by gene expression estimates the Arabidopsis GE 4X44K was first matched to the most recent Arabidopsis annotation, Araport11, by the BLAST algorithm. The results were analyzed using the limma R package. Here the background was correct with a moving minimum of 3 × 3 grids of spots and the expression was quantile normalized. DEGs (Padj. < 0.001) were placed in similarly regulated groups by calculating pairwise Euclidean distances followed by agglomerative hierarchical clustering using Ward's squared method. GO enrichment was determined with the GOstats R library.

Proteomics sample preparation and analysis

Plant growth material and conditions: Seedlings grown for proteomics harvests (*A. thaliana* seeds of ecotype Col-0) were sown in three rows at high density (~15–20 seeds/cm) on sterile square petri dishes containing 40 mL autoclaved and solidified 1/4 MS, 1% plant agar without additional sucrose, using a pipette after wet surface seed sterilization (incubation in 50% EtOH, 5% Bleach for 10 min, followed by seven washing rounds with Autoclaved MQ water). The plates were left to dry for 30 min after sowing. Petri dishes were sealed with gas-permeable tape (Leukopor, Duchefa) and stratified at 4°C in the dark for 4 days. Seedlings were grown vertically on the agar plates under short-day conditions (9:00–17:00, T = 20°C, Photon Flux Density = ~120 μmol $m^{-2}s^{-1}$, RH = 70%) for 5 days. Samples were harvested over five independent experiments; 10 plates were pooled per biological replicate. Air and ethylene treatments were performed as described above.

Sample preparation, tandem mass tag (TMT) labeling and data analysis: Protein extraction, quantification, reduction, and alkalization was done as described previously (Zhang et al., 2015). Protein precipitation was done by the methanol/chloroform method described by (Zhang et al., 2018). Sequential trypsin digestion was done according to (Zhang et al., 2015). Peptide concentration was determined using a PierceTM Quantitative Colorimetric Peptide Assay kit (23275; Thermo Fisher Scientific, Waltham, MA, USA). An aliquot of 100 μg peptide was labeled using TMT10plex (90110; Thermo Scientific). Five biological replicates were performed: Air-treated samples were labeled with TMT10-126, -127N, -127C, -128N, -128C, and ethylene-treated samples were labeled with -129 N, -129C, -130N, -130C, and -131. Peptides were mixed equally and an aliquot corresponding to half of peptides was separated by high pH reverse-phase chromatography using a Waters reverse-phase Nano column as described in Zhang et al. (2015). All LC-MS/MS experiments were performed as previously (Zhang et al., 2018) using a Dionex Ultimate 3000 RSLC nanoUPLC (Thermo Fisher Scientific Inc., Waltham, MA, USA) system and a Orbitrap Fusion Lumos Tribrid Mass Spectrometer (Thermo Fisher Scientific Inc., Waltham, MA, USA).

Raw data were searched against the TAIR10 database using MASCOT version 2.4 (Matrix Science, London, UK) and PROTEOME DISCOVERER version 1.4.1.14 as described previously (Zhang et al., 2015), employing Top 10 peaks filter node and percolator nodes and reporter ions quantifier with Trypsin enzyme specificity with a maximum of one missed cleavage. Carbamidomethylation (+57.021 Da) of cysteine and TMT isobaric labeling (+229.162 Da) of lysine and N-termini were set as static modifications while the methionine oxidation (+15.996) were considered dynamic. Mass tolerances were set to 20 ppm for MS and 0.6 Da for [A]MS/MS. For quantification, TMT 10plex method was used and integration tolerance was set to 2 mmu, Integration Method was set as centroid sum. Purity correction factors were set according to the TMT10plex (90110) product sheet (Lot number: SA239883). Each reporting ion was divided by the sum of total ions and normalized by medians of each sample. Log transformation ensured a homogeneity and normal distribution of the variances. Statistical differences between air and ethylene samples were obtained using two-sample *t* test of $\log_2$ transformed data, considering variation of quantification as a weighting factor. Only proteins represented by two or more peptides were considered for further analysis. All proteomics data is available in Supplemental Data Sets 8–10. MS proteomics data have been deposited to the ProteomeXchange Consortium via the PRIDE partner repository (Vizcaíno et al., 2016) with the dataset identifier PXD 031138. R language was used for Ontology (GO) enrichment analysis.

Downloaded from https://academic.oup.com/plphys/article/190/2/1365/6595039 by Erasmus University Library user on 29 September 2022

Antioxidant quantification

Glutathione and AA content were quantified using the GSH-GLO Glutathione Assay Kit (Promega, Madison, WI, USA) and Megazyme kit (K-ASCO 04/19, Wicklow, Ireland), respectively. Briefly, approximately 600 root tips were harvested per sample through flash freezing after treatment. The manufacturer's protocols were adapted for extraction and quantification as previously described (Yeung et al., 2018). Glutathione and AA values were normalized by total soluble protein content per sample. Protein content was measured using the Pierce BCA Protein Assay Kit (ThermoFisher).

Peroxidase activity was quantified using the Peroxidase Activity Assay Kit (Sigma-Aldrich). Briefly, appproximately 600 root tips were harvested per sample and rapidly homogenized with 100 mL of Assay Buffer. Sample supernatant (50 mL) was incubated with Peroxidase Master Reaction Mix (50 mL) in 96-well plate and incubated at 37°C for 10 min. Colorimetric measurements (absorbance at 570 nm) were performed every 3 min for a total time of 18 min and a standard curve (0–10 nmol H_2O_2) was included. Peroxidase activity was calculated by dividing the amount (nmol) of H_2O_2 reduced between $T_{initial}$ and T_{final} by the measuring time (18 min) and sample volume (100 mL).

H_2O_2 visualization

DAB staining: DAB is oxidized by H_2O_2 in the presence of peroxidases to generate a dark brown precipitate (Thordal-Christensen et al., 1997). Seedlings were incubated with 1 mg·mL^{-1} DAB (Sigma-Aldrich) in 20-mM 2-ethanesulfonic acid (MES; Sigma-Aldrich) buffer (pH 6.2) supplemented by 10 units·mL^{-1} peroxidase from horseradish (Sigma-Aldrich) for 1 h. Seedlings were then rinsed with MES buffer for 1 min twice before imaging (Dubreuil-Maurizi et al., 2011). Olympus BX50WI was used to visualize DAB staining and images were taken under 10× objective lens.

Confocal imaging of mt-roGFP2-Orp1: to visualize subcellular levels of H_2O_2, confocal imaging of 5-day-old *mt-roGFP2-Orp1* Arabidopsis seedlings was performed right after experimental time-points with a Zeiss Observer Z1 LSM700 confocal microscope (oil immersion, 40× objective Plan-Neofluar N.A. 1.30). RoGFP2-Orp1 was excited sequentially at 405 and 488 nm and emission was recorded at 505–535 nm. The 405/488 ratio within root tips was determined in similar areas of ~5,000 μm^2 using ICY software (http://icy.bioimageanalysis.org).

Statistical analyses

Data were analyzed in R software using a *t* test, or an ANOVA followed by Tukey's least significant difference (LSD) as post-hoc test. The EMMEANS package was used. In some cases, the data were log-transformed to adhere to the assumption required by the statistical test, such as a normal data distribution and evenly distributed error terms. Differences in survival (count data) were analyzed by generalized linear modeling using the binomial link function.

Accession numbers

Sequence data from this article can be found in the GenBank/EMBL data libraries under the accession numbers provided in the supplemental data.

Supplemental data

The following materials are available in the online version of this article.

Supplemental Table S1. The effect of ethylene on MC-protein abundance.

Supplemental Table S2. Comparison of identified proteins regulated by the PRT6 N-degron pathway and ethylene.

Supplemental Figure S1. Ethylene pretreatment improves root tip performance during hypoxia and re-oxygenation.

Supplemental Figure S2. Volcano plots of hypoxia and re-oxygenation transcriptome responses of ethylene and air pretreated seedlings.

Supplemental Figure S3. Volcano plots showing the difference between transcriptomes of ethylene and air pretreated seedlings over the course of the pretreatment, hypoxia, and re-oxygenation.

Supplemental Figure S4. Ethylene-specific transcript level responses during hypoxia and re-oxygenation.

Supplemental Figure S5. Transcript level changes that are independent of ethylene pretreatment.

Supplemental Figure S6. Several key ROS homeostasis gene families respond differently to ethylene treatment.

Supplemental Figure S7. Ethylene-mediated increase in HUPs might contribute to hypoxia survival of Arabidopsis root tips.

Supplemental Figure S8. Ethylene limits H_2O_2 accumulation during subsequent hypoxia and re-oxygenation.

Supplemental Figure S9. Ethylene rapidly slows down growth of primary roots.

Supplemental Data Set 1. Microarray and cluster membership.

Supplemental Data Set 2. GO enrichment pretreatment dependent clusters, BP.

Supplemental Data Set 3. GO enrichment pretreatment dependent clusters, MF.

Supplemental Data Set 4. GO enrichment pretreatment dependent clusters, CC.

Supplemental Data Set 5. GO enrichment pretreatment independent clusters, BP.

Supplemental Data Set 6. GO enrichment pretreatment independent clusters, MF.

Supplemental Data Set 7. GO enrichment pretreatment independent clusters, CC.

Supplemental Data Set 8. Identified proteins.

Supplemental Data Set 9. Identified proteins with multiple unique peptides.

Supplemental Data Set 10. GO enrichment among regulated proteins.

Supplemental Data Set 11. N-terminal MC-proteins.

Supplemental Data Set 12. mETC proteins.

Downloaded from https://academic.oup.com/plphys/article/190/2/1365/6595039 by Erasmus University Library user on 29 September 2022

Acknowledgments

We thank Malcolm Bennett and Bipin Pandey for providing seeds of *aux1-22* (Swarup et al., 2007), Angelika Mustroph for *rap2.2 rap2.12* and its WT background crosses (Gasch et al., 2016), Thomas Nietzel and Markus Schwarzländer for *mt-roGFP2-Orp1* (Nietzel et al., 2019) and Bram van de Poel for *eto1eol1eol2* (Christians et al., 2009). We acknowledge Dr. Michael J. Deery of Cambridge Centre for Proteomics, Cambridge University, for assistance with MS, Nienke van Dongen, Emilie Reinen, and Ankie Ammerlaan for technical support. The authors wish to dedicate this article to Femke Bosman, who passed away during the copy-editing of this article.

Funding

This work was supported by the Netherlands Organization for Scientific Research; 831.15.001 and 019.201EN.004 to S.H., 824.14.007 to L.A.C.J.V. and S.M., BB.00534.1 to R.S. and ALWOP.419 to Hv.V. and R.S. Z.L. was supported by a China Scholarship Council grant No. 201406300100. S.H. was also funded by the Deutsche Forschungsgemeinschaft (DFG, German Research Foundation) under Germany's Excellence Strategy (CIBSS–EXC-2189–Project ID 390939984). Research at Rothamsted was funded by Centre for Sustainable Intensification of Agriculture (CSIA) grant 18-6 awarded to H.Z. and the Biotechnology and Biological Sciences Research Council (BBSRC) Tailoring Plant Metabolism Institute Strategic Grant BBS/E/C/000I0420. M.H. and J.B.S were supported by US National Science Foundation (MCB-1716913).

Conflict of interest statement. None declared.

References

Aida M, Beis D, Heidstra R, Willemsen V, Blilou I, Galinha C, Nussaume L, Noh Y-S, Amasino R, Scheres B (2004) The PLETHORA genes mediate patterning of the Arabidopsis root stem cell niche. Cell **119**: 109–120

Alonso JM, Stepanova AN, Solano R, Wisman E, Ferrari S, Ausubel FM, Ecker JR (2003) Five components of the ethylene-response pathway identified in a screen for weak ethylene-insensitive mutants in Arabidopsis. Proc Natl Acad Sci USA **100**: 2992–2997

Arbona V, Hossain Z, López-Climent MF, Pérez-Clemente RM, Gómez-Cadenas A (2008) Antioxidant enzymatic activity is linked to waterlogging stress tolerance in citrus. Physiol Plant **132**: 452–466

Banga M, Slaa EJ, Blom C, Voesenek L (1996) Ethylene biosynthesis and accumulation under drained and submerged conditions (A comparative study of two rumex species). Plant Physiol **112**: 229–237

Bleecker AB, Estelle MA, Somerville C, Kende H (1988) Insensitivity to ethylene conferred by a dominant mutation in *Arabidopsis thaliana*. Science **241**: 1086–1089

Bui LT, Giuntoli B, Kosmacz M, Parlanti S, Licausi F (2015) Constitutively expressed ERF-VII transcription factors redundantly activate the core anaerobic response in *Arabidopsis thaliana*. Plant Sci **236**: 37–43

Chang KN, Zhong S, Weirauch MT, Hon G, Pelizzola M, Li H, Huang SC, Schmitz RJ, Urich MA, Kuo D, et al. (2013) Temporal transcriptional response to ethylene gas drives growth hormone cross-regulation in Arabidopsis. eLife **2**: e00675

Chang WWP, Huang L, Shen M, Webster C, Burlingame AL, Roberts JKM (2000) Patterns of protein synthesis and tolerance of anoxia in root tips of maize seedlings acclimated to a low-oxygen environment, and identification of proteins by mass spectrometry. Plant Physiol **122**: 295–317

Christians MJ, Gingerich DJ, Hansen M, Binder BM, Kieber JJ, Vierstra RD (2009) The BTB ubiquitin ligases ETO1, EOL1 and EOL2 act collectively to regulate ethylene biosynthesis in Arabidopsis by controlling type-2 ACC synthase levels. Plant J **57**: 332–345

Das K, Roychoudhury A (2014) Reactive oxygen species (ROS) and response of antioxidants as ROS-scavengers during environmental stress in plants. Front Environ Sci **2**: 53

Dubreuil-Maurizi C, Vitecek J, Marty L, Branciard L, Frettinger P, Wendehenne D, Meyer AJ, Mauch F, Poinssot B (2011) Glutathione deficiency of the Arabidopsis mutant pad2-1 affects oxidative stress-related events, defense gene expression, and the hypersensitive response. Plant Physiol **157**: 2000–2012

Ellis MH, Dennis ES, Peacock WJ (1999) Arabidopsis roots and shoots have different mechanisms for hypoxic stress tolerance. Plant Physiol **119**: 57–64

Foyer CH, Noctor G (2011) Ascorbate and glutathione: the heart of the redox hub. Plant Physiol **155**: 2–18

Fukao T, Yeung E, Bailey-Serres J (2011) The submergence tolerance regulator SUB1A mediates crosstalk between submergence and drought tolerance in rice. Plant Cell **23**: 412–427

Gahagan HE, Holm RE, Abeles FB (1968) Effect of ethylene on peroxidase activity. Physiol Plant **21**: 1270–1279

Galinha C, Hofhuis H, Luijten M, Willemsen V, Blilou I, Heidstra R, Scheres B (2007) PLETHORA proteins as dose-dependent master regulators of Arabidopsis root development. Nature **449**: 1053–1057

Gasch P, Fundinger M, Müller JT, Lee T, Bailey-Serres J, Mustroph A (2016) Redundant ERF-VII transcription factors bind to an evolutionarily conserved cis -motif to regulate hypoxia-responsive gene expression in Arabidopsis. Plant Cell **28**: 160–180

Gibbs DJ, Lee SC, Md Isa N, Gramuglia S, Fukao T, Bassel GW, Correia CS, Corbineau F, Theodoulou FL, Bailey-Serres J, et al. (2011) Homeostatic response to hypoxia is regulated by the N-end rule pathway in plants. Nature **479**: 415–418

Gibbs DJ, Md Isa N, Movahedi M, Lozano-Juste J, Mendiondo GM, Berckhan S, Marín-de la Rosa N, Vicente Conde J, Sousa Correia C, Pearce SP, et al. (2014) Nitric oxide sensing in plants is mediated by proteolytic control of group VII ERF transcription factors. Mol Cell **53**: 369–379

Gibbs DJ, Tedds HM, Labandera A-M, Bailey M, White MD, Hartman S, Sprigg C, Mogg SL, Osborne R, Dambire C, et al. (2018) Oxygen-dependent proteolysis regulates the stability of angiosperm polycomb repressive complex 2 subunit VERNALIZATION 2. Nat Commun **9**: 5438

Gill SS, Anjum NA, Hasanuzzaman M, Gill R, Trivedi DK, Ahmad I, Pereira E, Tuteja N (2013) Glutathione and glutathione reductase: a boon in disguise for plant abiotic stress defense operations. Plant Physiol Biochem **70**: 204–212

Gonzali S, Loreti E, Cardarelli F, Novi G, Parlanti S, Pucciariello C, Bassolino L, Banti V, Licausi F, Perata P (2015) Universal stress protein HRU1 mediates ROS homeostasis under anoxia. Nat Plants **1**: 1–9

Guo Y, Chen J, Kuang L, Wang N, Zhang G, Jiang L, Wu D (2020) Effects of waterlogging stress on early seedling development and transcriptomic responses in *Brassica napus*. Mol Breed **40**: 85

Hammond C, Mira MM, Ayele BT, Renault S, Hill RD, Stasolla C (2020) Over-expression of the *Zea mays* phytoglobin (ZmPgb1.1) alleviates the effect of water stress through shoot-specific mechanisms. Plant Physiol Biochem **155**: 384–395

Downloaded from https://academic.oup.com/plphys/article/190/2/1365/6595039 by Erasmus University Library user on 29 September 2022

Hartman S, van Dongen N, Renneberg DMHJ, Welschen-Evertman RAM, Kociemba J, Sasidharan R, Voesenek LACJ (2020) Ethylene differentially modulates hypoxia responses and tolerance across solanum species. Plants **9**: 1022

Hartman S, Liu Z, van Veen H, Vicente J, Reinen E, Martopawiro S, Zhang H, van Dongen N, Bosman F, Bassel GW, et al. (2019) Ethylene-mediated nitric oxide depletion pre-adapts plants to hypoxia stress. Nat Commun **10**: 1–9

Hartman S, Sasidharan R, Voesenek LACJ (2021) The role of ethylene in metabolic acclimations to low oxygen. New Phytol **229**: 64–70

Hebelstrup KH, Van Zanten M, Mandon J, Voesenek LACJ, Harren FJM, Cristescu SM, Møller IM, Mur LAJ (2012) Haemoglobin modulates NO emission and hyponasty under hypoxia-related stress in *Arabidopsis thaliana*. J Exp Bot **63**: 5581–5591

Hirabayashi Y, Mahendran R, Koirala S, Konoshima L, Yamazaki D, Watanabe S, Kim H, Kanae S (2013) Global flood risk under climate change. Nat Clim Chang **3**: 816–821

Holman TJ, Jones PD, Russell L, Medhurst A, Ubeda Tomas S, Talloji P, Marquez J, Schmuths H, Tung S-A, Taylor I, et al. (2009) The N-end rule pathway promotes seed germination and establishment through removal of ABA sensitivity in Arabidopsis. Proc Natl Acad Sci USA **106**: 4549–4554

Hong CP, Wang MC, Yang CY (2020) NADPH oxidase RbohD and ethylene signaling are involved in modulating seedling growth and survival under submergence stress. Plants **9**: 471

Huang X, Shabala L, Zhang X, Zhou M, Voesenek LACJ, Hartman S, Yu M, Shabala S (2022) Cation transporters in cell fate determination and plant adaptive responses to a low-oxygen environment. J Exp Bot **73**: 636–645

Juntawong P, Girke T, Bazin J, Bailey-Serres J (2014) Translational dynamics revealed by genome-wide profiling of ribosome footprints in Arabidopsis. Proc Natl Acad Sci USA **111**: E203–12

Kawa D, Meyer AJ, Dekker HL, Abd-El-Haliem AM, Gevaert K, Van De Slijke E, Maszkowska J, Bucholc M, Dobrowolska G, De Jaeger G, et al. (2020) SnRK2 protein kinases and mRNA decapping machinery control root development and response to salt. Plant Physiol **182**: 361–377

Le J, Vandenbussche F, Van Der Straeten D, Verbelen J-P (2001) In the early response of Arabidopsis roots to ethylene, cell elongation is up- and down-regulated and uncoupled from differentiation. Plant Physiol **125**: 519–522

Lee SC, Mustroph A, Sasidharan R, Vashisht D, Pedersen O, Oosumi T, Voesenek LACJ, Bailey-Serres J (2011) Molecular characterization of the submergence response of the *Arabidopsis thaliana* ecotype Columbia. New Phytol **190**: 457–471

Licausi F, Van Dongen JT, Giuntoli B, Novi G, Santaniello A, Geigenberger P, Perata P (2010) HRE1 and HRE2, two hypoxia-inducible ethylene response factors, affect anaerobic responses in *Arabidopsis thaliana*. Plant J **62**: 302–315

Licausi F, Kosmacz M, Weits DA, Giuntoli B, Giorgi FM, Voesenek LACJ, Perata P, van Dongen JT (2011) Oxygen sensing in plants is mediated by an N-end rule pathway for protein destabilization. Nature **479**: 419–422

Loreti E, van Veen H, Perata P (2016) Plant responses to flooding stress. Curr Opin Plant Biol **33**: 64–71

Mabuchi K, Maki H, Itaya T, Suzuki T, Nomoto M, Sakaoka S, Morikami A, Higashiyama T, Tada Y, Busch W, et al. (2018) MYB30 links ROS signaling, root cell elongation, and plant immune responses. Proc Natl Acad Sci USA **115**: E4710–E4719

Mao JL, Miao ZQ, Wang Z, Yu LH, Cai XT, Xiang CB (2016) Arabidopsis ERF1 mediates cross-talk between ethylene and auxin biosynthesis during primary root elongation by regulating ASA1 expression. PLoS Genet **12**: e1005760

McLoughlin F, Galvan-Ampudia CS, Julkowska MM, Caarls L, Van Der Does D, Laurière C, Munnik T, Haring MA, Testerink C (2012) The Snf1-related protein kinases SnRK2.4 and SnRK2.10 are involved in maintenance of root system architecture during salt stress. Plant J **72**: 436–449

Mehlhorn H (1990) Ethylene-promoted ascorbate peroxidase activity protects plants against hydrogen peroxide, ozone and paraquat. Plant Cell Environ **13**: 971–976

Miao ZQ, Zhao PX, Mao JL, Yu LH, Yuan Y, Tang H, Liu ZB, Xiang C Bin (2018) HOMEOBOX PROTEIN52 mediates the crosstalk between ethylene and auxin signaling during primary root elongation by modulating auxin transport-related gene expression. Plant Cell **30**: 2761–2778

Millar AH, Heazlewood JL, Giglione C, Holdsworth MJ, Bachmair A, Schulze WX (2019) The scope, functions, and dynamics of post-translational protein modifications. Annu Rev Plant Biol **70**: 119–151

Mira MM, Huang S, Hill RD, Stasolla C (2021) Tolerance to excess moisture in soybean is enhanced by over-expression of the *Glycine max* Phytoglobin (GmPgb1). Plant Physiol Biochem **159**: 322–334

Mithran M, Paparelli E, Novi G, Perata P, Loreti E (2014) Analysis of the role of the pyruvate decarboxylase gene family in *Arabidopsis thaliana* under low-oxygen conditions. Plant Biol **16**: 28–34

Mittler R (2017) ROS are good. Trends Plant Sci **22**: 11–19

Müssig C, Shin GH, Altmann T (2003) Brassinosteroids promote root growth in Arabidopsis. Plant Physiol **133**: 1261–1271

Mustroph A, Lee SC, Oosumi T, Zanetti ME, Yang H, Ma K, Yaghoubi-Masihi A, Fukao T, Bailey-Serres J (2010) Cross-kingdom comparison of transcriptomic adjustments to low-oxygen stress highlights conserved and plant-specific responses. Plant Physiol **152**: 1484–1500

Ni XL, Gui MY, Tan LL, Zhu Q, Liu WZ, Li CX (2019) Programmed cell death and aerenchyma formation in water-logged sunflower stems and its promotion by ethylene and ROS. Front Plant Sci **9**: 1928

Nietzel T, Elsässer M, Ruberti C, Steinbeck J, Ugalde JM, Fuchs P, Wagner S, Ostermann L, Moseler A, Lemke P, et al. (2019) The fluorescent protein sensor roGFP^2-Orp1 monitors *in vivo* H_2O_2 and thiol redox integration and elucidates intracellular H_2O_2 dynamics during elicitor-induced oxidative burst in Arabid. New Phytol **221**: 1649–1664

Pandey BK, Huang G, Bhosale R, Hartman S, Sturrock CJ, Jose L, Martin OC, Karady M, Voesenek LACJ, Ljung K, et al. (2021) Plant roots sense soil compaction through restricted ethylene diffusion. Science **371**: 276–280

Papdi C, Pérez-Salamõ I, Joseph MP, Giuntoli B, Bögre L, Koncz C, Szabados L (2015) The low oxygen, oxidative and osmotic stress responses synergistically act through the ethylene response factor VII genes RAP2.12, RAP2.2 and RAP2.3. Plant J **82**: 772–784

Peng HP, Chan CS, Shih MC, Yang SF (2001) Signaling events in the hypoxic induction of alcohol dehydrogenase gene in Arabidopsis. Plant Physiol **126**: 742–749

Peng J, Li Z, Wen X, Li W, Shi H, Yang L, Zhu H, Guo H (2014) Salt-induced stabilization of EIN3/EIL1 confers salinity tolerance by deterring ROS accumulation in Arabidopsis. PLoS Genet **10**: e1004664

Perata P (2020) Ethylene signaling controls fast oxygen sensing in plants. Trends Plant Sci **25**: 3–6

Pucciariello C, Parlanti S, Banti V, Novi G, Perata P (2012) Reactive oxygen species-driven transcription in Arabidopsis under oxygen deprivation. Plant Physiol **159**: 184–196

Qi X, Li Q, Ma X, Qian C, Wang H, Ren N, Shen C, Huang S, Xu X, Xu Q, et al. (2019) Waterlogging-induced adventitious root formation in cucumber is regulated by ethylene and auxin through reactive oxygen species signalling. Plant Cell Environ **42**: 1458–1470

Riber W, Müller JT, Visser EJW, Sasidharan R, Voesenek LACJ, Mustroph A (2015) The Greening after extended darkness1 is an N-end rule pathway mutant with high tolerance to submergence and starvation. Plant Physiol **167**: 1616–1629

Downloaded from https://academic.oup.com/plphys/article/190/2/1365/6595039 by Erasmus University Library user on 29 September 2022

Růžička K, Ljung K, Vanneste S, Podhorská R, Beeckman T, Friml J, Benková E (2007) Ethylene regulates root growth through effects on auxin biosynthesis and transport-dependent auxin distribution. Plant Cell **19**: 2197–2212

Sachs MM, Freeling M, Okimoto R (1980) The anaerobic proteins of maize. Cell **20**: 761–767

Sasidharan R, Hartman S, Liu Z, Martopawiro S, Sajeev N, van Veen H, Yeung E, Voesenek LACJ (2018) Signal dynamics and interactions during flooding stress. Plant Physiol **176**: 1106–1117

Sasidharan R, Voesenek LACJ (2015) Ethylene-mediated acclimations to flooding stress. Plant Physiol **169**: 3–12

Shi Z, Halaly-Basha T, Zheng C, Sharabi-Schwager M, Wang C, Galbraith DW, Ophir R, Pang X, Or E (2020) Identification of potential post-ethylene events in the signaling cascade induced by stimuli of bud dormancy release in grapevine. Plant J **104**: 1251–1268

Shimotohno A, Heidstra R, Blilou I, Scheres B (2018) Root stem cell niche organizer specification by molecular convergence of PLETHORA and SCARECROW transcription factor modules. Genes Dev **32**: 1085–1100

Skirycz A, Claeys H, de Bodt S, Oikawa A, Shinoda S, Andriankaja M, Maleux K, Eloy NB, Coppens F, Yoo SD, et al. (2011) Pause-and-stop: the effects of osmotic stress on cell proliferation during early leaf development in Arabidopsis and a role for ethylene signaling in cell cycle arrest. Plant Cell **23**: 1876–1888

Sozzani R, Cui H, Moreno-Risueno MA, Busch W, Van Norman JM, Vernoux T, Brady SM, Dewitte W, Murray JAH, Benfey PN (2010) Spatiotemporal regulation of cell-cycle genes by SHORTROOT links patterning and growth. Nature **466**: 128–132

Steffens B, Kovalev A, Gorb SN, Sauter M (2012) Emerging roots alter epidermal cell fate through mechanical and reactive oxygen species signaling. Plant Cell **24**: 3296–3306

Street IH, Aman S, Zubo Y, Ramzan A, Wang X, Shakeel SN, Kieber JJ, Schaller GE (2015) Ethylene inhibits cell proliferation of the Arabidopsis root meristem. Plant Physiol **169**: 338–350

Swarup R, Perry P, Hagenbeek D, Van Der Straeten D, Beemster GTS, Sandberg G, Bhalerao R, Ljung K, Bennett MJ (2007) Ethylene upregulates auxin biosynthesis in Arabidopsis seedlings to enhance inhibition of root cell elongation. Plant Cell **19**: 2186–2196

Tagliani A, Tran AN, Novi G, Di Mambro R, Pesenti M, Sacchi GA, Perata P, Pucciariello C (2020) The calcineurin β-like interacting protein kinase CIPK25 regulates potassium homeostasis under low oxygen in Arabidopsis. J Exp Bot **71**: 2678–2689

Thordal-Christensen H, Zhang Z, Wei Y, Collinge DB (1997) Subcellular localization of H2O2 in plants. H2O2 accumulation in papillae and hypersensitive response during the barley-powdery mildew interaction. Plant J **11**: 1187–1194

Tian Q, Reed JW (1999) Control of auxin-regulated root development by the *Arabidopsis thaliana* SHY2/IAA3 gene. Development **126**: 711–21

Tsai KJ, Chou SJ, Shih MC (2014) Ethylene plays an essential role in the recovery of Arabidopsis during post-anaerobiosis reoxygenation. Plant Cell Environ **37**: 2391–2405

Tsukagoshi H, Busch W, Benfey PN (2010) Transcriptional regulation of ROS controls transition from proliferation to differentiation in the root. Cell **143**: 606–616

Vanlerberghe G (2013) Alternative oxidase: a mitochondrial respiratory pathway to maintain metabolic and signaling homeostasis during abiotic and biotic stress in plants. Int J Mol Sci **14**: 6805–6847

Vaseva II, Qudeimat E, Potuschak T, Du Y, Genschik P, Vandenbussche F, Van Der Straeten D (2018) The plant hormone ethylene restricts Arabidopsis growth via the epidermis. Proc Natl Acad Sci USA **115**: E4130–E4139

Vashisht D, Hesselink A, Pierik R, Ammerlaan JMH, Bailey-Serres J, Visser EJW, Pedersen O, van Zanten M, Vreugdenhil D, Jamar DCL, et al. (2011) Natural variation of submergence tolerance among *Arabidopsis thaliana* accessions. New Phytol **190**: 299–310

van Veen H, Mustroph A, Barding GA, Eijk MV, Welschen-Evertman RAM, Pedersen O, Visser EJW, Larive CK, Pierik R, Bailey-Serres J, et al. (2013) Two rumex species from contrasting hydrological niches regulate flooding tolerance through distinct mechanisms. Plant Cell **25**: 4691–4707

van Veen H, Vashisht D, Akman M, Girke T, Mustroph A, Reinen E, Hartman S, Kooiker M, van Tienderen P, Schranz ME, et al. (2016) Transcriptomes of eight *Arabidopsis thaliana* accessions reveal core conserved, genotype- and organ-specific responses to flooding stress. Plant Physiol **172**: 668–689

Vicente J, Mendiondo GM, Movahedi M, Peirats-Llobet M, Juan Y ting, Shen Y yen, Dambire C, Smart K, Rodriguez PL, Charng Y yung, et al. (2017) The cys-arg/N-end rule pathway is a general sensor of abiotic stress in flowering plants. Curr Biol **27**: 3183–3190.e4

Visser EJW, Pierik R (2007) Inhibition of root elongation by ethylene in wetland and non-wetland plant species and the impact of longitudinal ventilation. Plant Cell Environ **30**: 31–38

Vizcaíno JA, Csordas A, Del-Toro N, Dianes JA, Griss J, Lavidas I, Mayer G, Perez-Riverol Y, Reisinger F, Ternent T, et al. (2016) 2016 update of the PRIDE database and its related tools. Nucleic Acids Res **44**: D447–D456

Voesenek LACJ, Bailey-Serres J (2015) Flood adaptive traits and processes: an overview. New Phytol **206**: 57–73

Voesenek LACJ, Sasidharan R (2013) Ethylene – and oxygen signalling – drive plant survival during flooding. Plant Biol **15**: 426–435

Wu L, Zhang Z, Zhang H, Wang XC, Huang R (2008) Transcriptional modulation of ethylene response factor protein JERF3 in the oxidative stress response enhances tolerance of tobacco seedlings to salt, drought, and freezing. Plant Physiol **148**: 1953–1963

Yamauchi T, Watanabe K, Fukazawa A, Mori H, Abe F, Kawaguchi K, Oyanagi A, Nakazono M (2014) Ethylene and reactive oxygen species are involved in root aerenchyma formation and adaptation of wheat seedlings to oxygen-deficient conditions. J Exp Bot **65**: 261–273

Yang CY, Hong CP (2015) The NADPH oxidase Rboh D is involved in primary hypoxia signalling and modulates expression of hypoxia-inducible genes under hypoxic stress. Environ Exp Bot **115**: 63–72

Yeung E, Bailey-Serres J, Sasidharan R (2019) After the deluge: plant revival post-flooding. Trends Plant Sci **24**: 443–454

Yeung E, van Veen H, Vashisht D, Sobral Paiva AL, Hummel M, Rankenberg T, Steffens B, Steffen-Heins A, Sauter M, de Vries M, et al. (2018) A stress recovery signaling network for enhanced flooding tolerance in *Arabidopsis thaliana*. Proc Natl Acad Sci USA **115**: E6085–E6094

Yoshida S, Tamaoki M, Ioki M, Ogawa D, Sato Y, Aono M, Kubo A, Saji S, Saji H, Satoh S, et al. (2009) Ethylene and salicylic acid control glutathione biosynthesis in ozone-exposed *Arabidopsis thaliana*. Physiol Plant **136**: 284–298

Youssef MS, Mira MM, Renault S, Hill RD, Stasolla C (2016) Phytoglobin expression influences soil flooding response of corn plants. Ann Bot **118**: 919–931

Zhang H, Deery MJ, Gannon L, Powers SJ, Lilley KS, Theodoulou FL (2015) Quantitative proteomics analysis of the Arg/N-end rule pathway of targeted degradation in Arabidopsis roots. Proteomics **15**: 2447–2457

Zhang H, Gannon L, Hassall KL, Deery MJ, Gibbs DJ, Holdsworth MJ, van der Hoorn RAL, Lilley KS, Theodoulou FL (2018) N-terminomics reveals control of Arabidopsis seed storage proteins and proteases by the Arg/N-end rule pathway. New Phytol **218**: 1106–1126

Downloaded from https://academic.oup.com/plphys/article/190/2/1365/6595039 by Erasmus University Library user on 29 September 2022